Delft University of Technology

Delft Center for Systems and Control

Technical report 16-026

A mesoscopic integrated urban traffic flow-emission model*

A. Jamshidnejad, I. Papamichail, M. Papageorgiou, and
B. De Schutter

If you want to cite this report, please use the following reference instead:
A. Jamshidnejad, I. Papamichail, M. Papageorgiou, and B. De Schutter, "A mesoscopic integrated urban traffic flow-emission model," *Transportation Research Part C*, vol. 75, pp. 45–83, Feb. 2017.

Delft Center for Systems and Control
Delft University of Technology
Mekelweg 2, 2628 CD Delft
The Netherlands
phone: +31-15-278.24.73 (secretary)
URL: `https://www.dcsc.tudelft.nl`

*This report can also be downloaded via `https://pub.deschutter.info/abs/16_026.html`

A mesoscopic integrated urban traffic flow-emission model

Anahita Jamshidnejad*, Ioannis Papamichail†, Markos Papageorgiou†, Bart De Schutter*

Abstract

Due to the noticeable environmental and economical problems caused by traffic congestion and by the emissions produced by traffic, analysis and control of traffic is essential. One of the various traffic analysis approaches is the model-based approach, where a mathematical model of the traffic system is developed/used based on the governing physical rules of the system. In this paper, we propose a framework to interface and integrate macroscopic flow models and microscopic emission models. As a result, a new mesoscopic integrated flow-emission model is obtained that provides a balanced trade-off between high accuracy and low computation time. The proposed approach considers an aggregated behavior for different groups of vehicles (mesoscopic) instead of considering the behavior of individual vehicles (microscopic) or the entire group of vehicles (macroscopic). A case study is done to evaluate the proposed framework, considering the performance of the resulting mesoscopic integrated flow-emission model. The traffic simulation software SUMO combined with the microscopic emission model VT-micro is used as the comparison platform. The results of the case study prove that the proposed approach provides excellent results with high accuracy levels. In addition, the mesoscopic nature of the integrated flow-emission model guarantees a low CPU time, which makes the proposed framework suitable for real-time model-based applications.

1 Introduction

Emissions produced by vehicles in urban traffic areas, especially when traffic becomes congested and vehicles start to idle in long queues, significantly increase the level of harmful substances in the air such as carbon monoxide (CO) and dioxide (CO_2), hydrocarbon (HC), and nitrogen oxides (NO_x) (Sjodin et al., 1998; Anderson et al., 1996; Barth and Boriboonsomsin, 2008; Barth et al., 1996). This may be dangerous, especially in sensitive urban areas, e.g., in the neighborhood of hospitals, nursing homes for the elderly people, schools, etc. Additionally, another consequence of congested urban traffic is increased fuel consumption and the expenses it imposes on societies. According to a report published by the Center for Economics and Business Research (2014), the expected costs caused by traffic in the UK, US, Germany, and France might increase by up to 46 % by 2030 w.r.t. 2013.

To mitigate the problems regarding increased emissions and fuel consumption in urban traffic networks, model-based analysis and control may be used. Model-predictive control (MPC) (Maciejowski, 2002) is a model-based control approach that has proven to be efficient for traffic networks (see (Diakaki et al., 2002, 2003; Aboudolas et al., 2010; van den Berg et al., 2007; Bellemans et al., 2006) for the application of MPC in urban

*Delft Center for Systems and Control (DCSC), Delft University of Technology, the Netherlands
†Dynamic Systems & Simulation Laboratory, Technical University of Crete, Greece

traffic networks and freeways). Therefore, from an environmental and an economical point-of-view, it is important to develop and to improve urban emission models that give an estimate of the current and possible future emission and fuel consumption levels.

Based on the level of detail, different traffic models (including flow and emission models) can be categorized as microscopic, mesoscopic, and macroscopic. If the model is focused on more details and takes into account the behavior of individual vehicles in the network, it is called a microscopic traffic model (Pipes, 1953; Gazis et al., 1961; Qi et al., 2004). Some traffic models express the average behavior of the vehicles as a fluid. These models are known as macroscopic traffic models (see e.g. (Messmer and Papageorgiou, 1990; Ntziachristos et al., 2009)). There is also a third category for traffic models, known as mesoscopic models (Hoogendoorn and Bovy, 2001), which partly use the characteristics of microscopic and macroscopic models, i.e., the level of detail for a mesoscopic model is less than a microscopic and greater than a macroscopic traffic model.

The focus of this paper is on the introduction and development of a new framework for integrating and interfacing any macroscopic urban traffic flow model that updates the total number of vehicles in the links and the number of vehicles standing in the queues as the states of the traffic network (e.g., the S-model by Lin et al. (2012)) with any microscopic emission model that uses both the speed and the acceleration of the individual vehicles in order to compute the emission and the fuel consumption levels (e.g., VT-micro by Ahn et al. (1999) and VERSIT+ by Ligterink et al. (2009)). The proposed approach will result in a new mesoscopic integrated urban traffic flow-emission model that provides a balanced trade-off between high accuracy and low computation time. The resulting model belongs to the mesoscopic category considering the following characteristic given for mesoscopic traffic models by Hoogendoorn and Bovy (2001); mesoscopic models specify the behavior of traffic by groups of vehicles/drivers, were the interactions of these vehicles/drivers are described in a low level of detail.

In order to compute the emission levels, several models from different classes (i.e., microscopic, mesoscopic, and macroscopic) have been developed (e.g., see the macroscopic models by Ntziachristos et al. (2009) and by Csikós et al. (2015), the mesoscopic models by Rakha et al. (2011) and by Gori et al. (2013), and the microscopic models by Ahn et al. (1999), by Ligterink et al. (2009), and by Chen and Yu (2007)).

Some macroscopic models provide a high computation speed (such as COPERT, which is based on the average speed of the vehicles by Ntziachristos et al. (2009) and the macroscopic model based on the total travel distance and the average speed by (Csikós et al., 2015)), while they ignore the effect of acceleration and deceleration of the vehicles. This may bring issues for the accuracy of the results, especially in urban traffic areas with signalized intersections. More specifically, experiments show that in case of positive acceleration, and in particular for the emissions of NO_x, the minimum of the emissions (in g/km) as a function of speed does not always correspond to the urban traffic free-flow speed. Hence, minimizing the total delays of the vehicles does not necessarily lead to minimization of the emissions. Hence, in our proposed framework, we take into account the effect of the acceleration and deceleration of the vehicles to improve the accuracy of the results for urban traffic networks.

The mesoscopic model developed by Rakha et al. (2011) provides promising results w.r.t. the microscopic model VT-micro (the errors are within the range of 10-27 %). In the current paper, we aim to improve the accuracy of these results to an even higher level for a mesoscopic model that is resulting from our proposed integrating framework. Hence, we start from a microscopic point-of-view, by considering the time-speed trajectories of individual vehicles in the traffic network. Then we distinct some groups of vehicles

with similar traffic behaviors and we define a (possibly virtual) representative vehicle for each group. Afterwards, we use a microscopic emission model (such as VT-micro or VERSIT+ to compute the instantaneous emissions of the representative vehicle for each specific traffic behavior (free-flow, idling, decelerating, accelerating). By multiplying the resulting emissions by the total number of vehicles in each group and by the average time of the given behavior, we obtain a mesoscopic emission model.

The simulation results show that the relative error of the computed emissions by our proposed mesoscopic approach are less than 6 %. Hence, we have successfully improved the results w.r.t. (Rakha et al., 2011). Compared with the mesoscopic model proposed by Gori et al. (2013), which is limited to signalized intersections and ignores the decelerating behavior of the vehicles, our framework is more general and can be used for both signalized and non-signalized traffic networks. As mentioned earlier, we do not ignore the decelerating behavior by the vehicles. Gori et al. (2013) consider two different traffic scenarios in an urban traffic network, i.e., the under-saturated and the saturated scenarios. We add a third scenario, i.e., the over-saturated scenario, which helps us to provide more accuracy.

Chen and Yu (2007) develop a microscopic simulation platform by integrating the microscopic traffic simulation VISSIM and the microscopic modal emission model CMEM. The aim of their work is to mostly provide a platform to assess the effect of different aspects in a traffic network on the amount of emissions. Our focus in this paper is mostly on providing a mathematical model for computation of emissions that can be applied in model-based analysis and control of traffic.

Previous work on integrating traffic flow and emission models includes the work by Zegeye et al. (2011), where METANET (Messmer and Papageorgiou, 1990), a macroscopic freeway flow model, and VT-micro is are integrated. For urban traffic, an integrated flow and emission model has been developed by Lin et al. (2013), where the S-model is integrated with VT-micro to form a simple integrated model that suits real-time control applications. The proposed macroscopic model has a low computation time and in a case study given in (Lin et al., 2013) shows satisfactory results when used as the internal model of a model-predictive controller. Inspired by the macroscopic integrated model given by Lin et al. (2013) and by Zegeye et al. (2011), in the current paper we develop a general mesoscopic framework to integrate macroscopic traffic flow models and microscopic emission models (i.e., our proposed framework is not limited to specific flow and emission models). The aim is to provide even more accuracy, while keeping the computation speed still high. Therefore, similar to the work by Lin et al. (2013), we divide the possible traffic states in an urban traffic network into three different scenarios, i.e., under-saturated, saturated, and over-saturated. In addition to that, we distinguish different groups of vehicles that may be observed for each traffic scenario. Hence, compared with the macroscopic model proposed by Lin et al. (2013), we build up a mesoscopic framework that takes into account more details than a macroscopic one. Moreover, we define a (possibly virtual) representative vehicle that should reflect an average behavior for all the vehicles in a group. In summary, our proposed framework provides more details compared with the previous work, while it still guarantees a trade-off between high accuracy and low computation time.

The rest of the paper is organized as follows; noting that the mesoscopic interfacing and integrating framework introduced in this paper is applicable to different flow and emission models, Section 2 discusses, as an example for the flow and emission models that may be integrated using the proposed framework, the S-model and VT-micro. In Section 3, we give general formulations to compute the emissions using instantaneous speed

and acceleration of the vehicles for different traffic behaviors in urban traffic networks. Sections 4, 5, and 6 present formulations for adapting the equations given in Section 3 for different urban traffic scenarios (i.e., under-saturated, saturated, and over-saturated scenarios). Section 7 presents the results of some test examples. The traffic simulation software SUMO is used to extract the traffic states. The instantaneous emissions per vehicle are computed by VT-micro. The results are compared with the emissions found via the new mesoscopic integrated flow-emission model. Section 8 concludes the work and gives topics for future work.

Contributions of the paper

The main contributions of the paper include:

1. We give a general framework for emission models including formulations for computing the instantaneous emissions for different traffic behaviors observed in a traffic network (e.g., uniform speed, accelerating, decelerating, etc.), applying microscopic models that use speed and/or acceleration of vehicles.

2. For urban traffic networks, we distinguish different possible traffic scenarios (including under-saturated, saturated, and over-saturated) within a mesoscopic structure. Then we separate different groups of vehicles that may be observed for each scenario. The distinction is based on the traffic behavior each group of vehicles show within the network. Time-speed curves are extracted for different groups of vehicles for each traffic scenario, where the curve represents the average behavior of the vehicles in that group for a (possibly virtual) representative vehicle.

3. We extract the formulas that compute the time spent and the emissions of the representative vehicle of each group, which, multiplied by the total number of vehicles within the group, gives the total time spent and the total emissions of the vehicles in that group.

2 Flow and emission model basis

The interfacing and integrating framework proposed in this paper results in a mesoscopic flow and emission model, where the proposed integrating approach is applicable to any macroscopic flow model that updates at every simulation time step the total number of vehicles observed in a link and the number of vehicles waiting in the queue in a link, and also any microscopic emission model that computes the emissions and/or fuel consumption of the vehicles in a network based on their individual instantaneous speed and acceleration. In this section, as one possible option, we describe the macroscopic urban traffic flow model, S-model (Lin et al., 2012) for computation of flow, and the microscopic emission model VT-micro (Ahn et al., 1999) for computation of emissions and fuel consumption.

The S-model is a nonlinear macroscopic urban traffic flow model that updates the total number of vehicles, $n_{u,d}(k_d)$, on a link (u,d) between an upstream intersection u and a downstream intersection d, and also the number of vehicles, $q_{u,d}(k_d)$, standing in a queue on the link at every simulation time step k_d by

$$n_{u,d}(k_d+1) = n_{u,d}(k_d) + \left(\alpha_{u,d}^{\text{enter,l}}(k_d) - \alpha_{u,d}^{\text{leave,l}}(k_d)\right) c_d, \tag{1}$$

$$q_{u,d}(k_d) = \sum_{o \in \mathcal{O}_{(u,d)}} q_{u,d,o}(k_d), \tag{2}$$

with

$$q_{u,d,o}(k_d+1) = q_{u,d,o}(k_d) + \left(\alpha^{\text{arrive,q}}_{u,d,o}(k_d) - \alpha^{\text{leave,l}}_{u,d,o}(k_d)\right) c_d, \tag{3}$$

where the definition of the notations given in the update equations are as follows[1] :

- c_d, the cycle time of the downstream intersection d, which is considered as the simulation sampling time for link (u,d),
- $\alpha^{\text{enter,l}}_{u,d}(k_d)$, the average entering flow rate for link (u,d) during $[k_d c_d, (k_d+1)c_d)$.
- $\alpha^{\text{leave,l}}_{u,d}(k_d)$, the average exiting flow rate for link (u,d) during $[k_d c_d, (k_d+1)c_d)$.
- $q_{u,d,o}(k_d)$, the number of those vehicles standing in the queue of link (u,d) that intend to turn towards the node o.
- $\alpha^{\text{arrive,q}}_{u,d,o}(k_d)$, the average value of the arriving flow rate at the tail of the waiting queue during $[k_d c_d, (k_d+1)c_d)$ that intend to turn towards the node o (note that in case the queue has fully been resolved, this quantity will be defined as the average value of the arriving flow rate at the end of the link instead of the queue).
- $\alpha^{\text{leave,l}}_{u,d,o}(k_d)$, the average value of the leaving flow rate during $[k_d c_d, (k_d+1)c_d)$ corresponding to the traffic sub-stream that intends to turn towards the node o.

VT-micro is a microscopic model that computes the instantaneous emissions of different substances such as CO, HC, and NO_x, and also the fuel consumption of vehicles based on their individual speed and acceleration. Suppose that for vehicle i, the observed values of the instantaneous speed and acceleration at time instant t are denoted by $v_i(t)$ and $a_i(t)$, respectively. First, we construct two vectors $\tilde{\boldsymbol{v}}(t)$ and $\tilde{\boldsymbol{a}}(t)$ of dimension 4, which are defined by

$$\begin{aligned} \tilde{\boldsymbol{v}}_i(t) &= \begin{bmatrix} 1 & v_i(t) & {v_i}^2(t) & {v_i}^3(t) \end{bmatrix}^\top, \\ \tilde{\boldsymbol{a}}_i(t) &= \begin{bmatrix} 1 & a_i(t) & {a_i}^2(t) & {a_i}^3(t) \end{bmatrix}^\top. \end{aligned} \tag{4}$$

The instantaneous emission of the substance e by vehicle i at time instant t is

$$E_{e,i}(t) = \exp\left(\tilde{\boldsymbol{v}}_i^\top(t) \cdot P_e \cdot \tilde{\boldsymbol{a}}_i(t)\right), \tag{5}$$

where P_e are 4×4 matrices, which are given by Zegeye (2011), for computing the emissions in [kg/s] or the fuel consumption in [l/s].

3 General framework for emission models

In this section, we integrate the S-model with an available microscopic emission model that produces instantaneous emissions $E_{e,i,u,d}(k_d)$ of substance e for vehicle i on link (u,d). In the end, we will see that the developed mesoscopic integrated model can admit any urban traffic flow model that produces the number of vehicles and the queue lengths on different links, and any microscopic emission model that computes the instantaneous emissions at time step k as a function of instantaneous speeds and accelerations of vehicles, i.e.,

$$E_{e,i,u,d}(k_d) = E_{e,i}\left(v_i(k_d), a_i(k_d)\right), \tag{6}$$

with $e \in \mathbb{E}$, and $\mathbb{E}$ the set including fuel consumption and polluting substances that are taken into account by the model.

To use (6), we need to extract $v_i(k)$ and $a_i(k)$ from the urban traffic flow model for groups of vehicles (traffic streams) that show a similar behavior. We first categorize different driving behaviors observed in urban traffic networks for different traffic scenarios.

[1]The superscript "l" stands for link, and the superscript "q" stands for queue.

3.1 Traffic behaviors for urban networks

We simplify the possible driving behaviors that might be observed for vehicles in parts of the simulation time slot and in different urban traffic scenarios via the following categories:

1. **Free-flow behavior**, for which the traffic stream moves with the free-flow speed $v_{u,d}^{\text{free}}$ on link (u, d), and $a_{u,d}^{\text{free}} = 0$.

2. **Idling behavior**, for which the traffic stream is waiting in a queue; we assume that the vehicles have a constant speed $v_{u,d}^{\text{idling}}$, and $a_{u,d}^{\text{idling}} = 0$.

3. **Decelerating behavior**, for which the traffic stream decreases its speed from $v_{u,d}^{b_1}$ to $v_{u,d}^{b_2}$ with a constant deceleration $a_{u,d}^{\text{dec}}$, with $b_1 \in \{\text{free}, \text{middle}\}$ and $b_2 \in \{\text{middle}, \text{idling}\}$, and $b_1 \neq b_2$.

4. **Accelerating behavior**, for which the traffic stream increases its speed from $v_{u,d}^{b_2}$ to $v_{u,d}^{b_1}$ with a constant acceleration[2] $a_{u,d}^{\text{acc}}$, with $b_1 \in \{\text{free}, \text{middle}\}$ and $b_2 \in \{\text{middle}, \text{idling}\}$, and $b_1 \neq b_2$.

5. **Nonstop behavior**, for which the traffic stream that has had a free-flow behavior during the current cycle, faces a green light at the end of the cycle. For a nonstop traffic behavior, two different reactions by the drivers might be observed:

   - In case the number of vehicles on the road is relatively low, as the traffic stream approaches the green light it might increase its speed from $v_{u,d}^{\text{free}}$ to $v_{u,d}^{\text{free}+}$ by a constant acceleration $a_{u,d}^{\text{acc}}$. This situation actually indicates that the ratio of the arriving flow at the end of the link, $\alpha_{u,d}^{\text{arrive,q}}(k_d)$, and the saturated average leaving flow, $\mu_{u,d}$, is less than or equal to a predefined threshold, $\lambda_{u,d}$. Hence,

   $$\frac{\alpha_{u,d}^{\text{arrive,q}}(k_d)}{\mu_{u,d}} \leq \lambda_{u,d},$$

   with $\lambda_{u,d}$ a threshold in $[0, 1]$. The parameter $\lambda_{u,d}$ can be determined via offline model identification using real-life data sets or data from a traffic microsimulator (Paz et al., 2015).

   - In case the number of vehicles on the road is relatively high, as the traffic stream approaches the green light it might decrease its speed from $v_{u,d}^{\text{free}}$ to $v_{u,d}^{\text{free}-}$ by a constant deceleration $a_{u,d}^{\text{dec}}$. Mathematically, this situation can be formulated by

   $$\frac{\alpha_{u,d}^{\text{arrive,q}}(k_d)}{\mu_{u,d}} > \lambda_{u,d}.$$

In the following section, we formulate the instantaneous emissions for each of the above behaviors, using the microscopic emission model given by (6). Note that since the nature of a nonstop behavior is either an accelerating or a decelerating behavior, we do not distinguish the nonstop behavior from the accelerating/decelerating behaviors in the following discussions.

[2]The acceleration and deceleration in this paper will adopt signed numbers, i.e., $a_{u,d}^{\text{dec}} < 0$ and $a_{u,d}^{\text{acc}} > 0$.

3.2 Emissions for different traffic behaviors

- Total emissions of $e \in \mathbb{E}$ caused by free-flow behavior on link (u,d) within the interval $\mathbb{I}_{u,d}^{\text{free}}(k_d)$, with $\mathbb{I}_{u,d}^{\text{free}}(k_d)$ the union of all sub-intervals of $[k_d c_d, (k_d+1)c_d)$, for which at least one vehicle on the link shows a free-flow behavior, is given by[3]:

$$\bar{E}_{e,u,d}^{\text{free}}(k_d) = \sum_{j=1}^{N_{u,d}^{\text{free}}(k_d)} \left(n_{u,d}^{\text{free},j}(k_d) T_{u,d}^{\text{free},j}(k_d) \right) \cdot E_e \left(v_{u,d}^{\text{free}}, 0 \right), \tag{7}$$

where $N_{u,d}^{\text{free}}(k_d)$ denotes the number of all sub-intervals $\mathbb{I}_{u,d}^{\text{free},j}(k_d)$ of $[k_d c_d, (k_d + 1)c_d)$, during which free-flow behavior is observed (i.e., $\mathbb{I}_{u,d}^{\text{free}}(k_d) = \bigcup_j \mathbb{I}_{u,d}^{\text{free},j}(k_d)$), and $n_{u,d}^{\text{free},j}(k_d)$ is the total number of vehicles that show a free-flow behavior within $\mathbb{I}_{u,d}^{\text{free},j}(k_d)$, and $T_{u,d}^{\text{free},j}(k_d)$ is the length of $\mathbb{I}_{u,d}^{\text{free},j}(k_d)$.

- Total emissions of $e \in \mathbb{E}$ caused by idling behavior on link (u,d) within the interval $\mathbb{I}_{u,d}^{\text{idling}}(k_d)$, with $\mathbb{I}_{u,d}^{\text{idling}}(k_d)$ the union of all sub-intervals of $[k_d c_d, (k_d+1)c_d)$, for which at least one vehicle on the link shows an idling behavior, is given by:

$$\bar{E}_{e,u,d}^{\text{idling}}(k_d) = \sum_{j=1}^{N_{u,d}^{\text{idling}}(k_d)} \left(n_{u,d}^{\text{idling},j}(k_d) T_{u,d}^{\text{idling},j}(k_d) \right) \cdot E_e \left(v_{u,d}^{\text{idling}}, 0 \right), \tag{8}$$

where $N_{u,d}^{\text{idling}}(k_d)$ denotes the number of all sub-intervals $\mathbb{I}_{u,d}^{\text{idling},j}(k_d)$ of $[k_d c_d, (k_d + 1)c_d)$, during which idling behavior is observed, and $n_{u,d}^{\text{idling},j}(k_d)$ is the total number of vehicles that show an idling behavior within $\mathbb{I}_{u,d}^{\text{idling},j}(k_d)$, and $T_{u,d}^{\text{idling},j}(k_d)$ is the length of $\mathbb{I}_{u,d}^{\text{idling},j}(k_d)$.

- Total emissions of $e \in \mathbb{E}$ caused by decelerating behavior on link (u,d) within the interval $\mathbb{I}_{u,d}^{\text{dec}}(k_d)$, with $\mathbb{I}_{u,d}^{\text{dec}}(k_d)$ the union of all sub-intervals of $[k_d c_d, (k_d+1)c_d)$, for which at least one vehicle on the link shows a decelerating behavior, is given by:

$$\bar{E}_{e,u,d}^{\text{dec}}(k_d) = \sum_{j=1}^{N_{u,d}^{\text{dec}}(k_d)} n_{u,d}^{\text{dec},j}(k_d) \cdot \int_{\mathbb{I}_{u,d}^{\text{dec},j}(k_d)} E_e \left(v(t), a_{u,d}^{\text{dec}} \right) \cdot \mathrm{d}t, \tag{9}$$

where $N_{u,d}^{\text{dec}}(k_d)$ denotes the number of all sub-intervals $\mathbb{I}_{u,d}^{\text{dec},j}(k_d)$ of $[k_d c_d, (k_d+1)c_d)$, during which a decelerating behavior is observed (i.e., $\mathbb{I}_{u,d}^{\text{dec}}(k_d) = \bigcup_j \mathbb{I}_{u,d}^{\text{dec},j}(k_d)$), $n_{u,d}^{\text{dec},j}(k_d)$ is the number of vehicles that show a decelerating behavior within $\mathbb{I}_{u,d}^{\text{dec},j}(k_d)$, and $T_{u,d}^{\text{dec},j}(k_d)$ is the length of $\mathbb{I}_{u,d}^{\text{dec},j}(k_d)$. Suppose that:

$$\mathbb{I}_{u,d}^{\text{dec},j}(k_d) = \left[t_{u,d}^{b_1,j}, t_{u,d}^{b_2,j} \right], \qquad j \in \{1, \ldots, N_{u,d}^{\text{dec}}(k_d)\},$$

then by changing the variable of integral from time t to speed v (knowing that

[3] To ease the notation, the subscript i is eliminated from (7) and following equations in this section.

$\mathrm{d}v = a_{u,d}^{\mathrm{dec}} \cdot \mathrm{d}t$), we obtain:

$$\begin{aligned} \bar{E}_{e,u,d}^{\mathrm{dec}}(k_d) &= \sum_{j=1}^{N_{u,d}^{\mathrm{dec}}(k_d)} n_{u,d}^{\mathrm{dec},j}(k_d) \cdot \int_{t_{u,d}^{b_1,j}}^{t_{u,d}^{b_2,j}} E_e\left(v(t), a_{u,d}^{\mathrm{dec}}\right) \cdot \mathrm{d}t \\ &= \sum_{j=1}^{N_{u,d}^{\mathrm{dec}}(k_d)} \frac{n_{u,d}^{\mathrm{dec},j}(k_d)}{a_{u,d}^{\mathrm{dec}}} \cdot \int_{v_{u,d}^{b_1,j}}^{v_{u,d}^{b_2,j}} E_e\left(v, a_{u,d}^{\mathrm{dec}}\right) \cdot \mathrm{d}v, \end{aligned} \tag{10}$$

with $v_{u,d}^{b_1}$ and $v_{u,d}^{b_2}$ the speed of the decelerating vehicles in $\mathbb{I}_{u,d}^{\mathrm{dec},j}(k_d)$ at, respectively, $t_{u,d}^{b_1}$ and $t_{u,d}^{b_2}$, and with $\{b_1 = \text{free} \wedge b_2 = \text{middle}\} \vee \{b_1 = \text{middle} \wedge b_2 = \text{idling}\} \vee \{b_1 = \text{free} \wedge b_2 = \text{idling}\} \vee \{b_1 = \text{free} \wedge b_2 = \text{nonstop} : \text{heavy}\}$.

- Total emissions caused by accelerating behavior on link (u, d) can be computed using a similar approach as we used for the decelerating behavior.

In the next sections (4, 5, and 6), we consider the following three traffic scenarios that might happen in an urban traffic network:

- under-saturated scenario,
- saturated scenario,
- over-saturated scenario.

For each of the above scenarios, we distinguish different groups of vehicles based on the traffic behaviors observed (see Section 3.1 for potential traffic behaviors). The traffic behavior of each group of vehicles is then illustrated via a time-speed curve, where this curve represents the behavior of a single representative vehicle, which shows the average collective behavior of that group. We define this average behavior as follows; since vehicles in each group will enter the link at different time instants, the starting time of the average time-speed curve is considered as the mid-point of the starting times of the curves corresponding to the first and the last vehicle in that group. Therefore, the time-speed curve corresponding to the representative vehicle illustrates the average time spent on a specific behavior that might be observed for each vehicle in that group. Later on, by computing the total number of vehicles in each group, i.e., the number of vehicles that will more or less follow the average time-speed behavior of the representative vehicles, we can find an estimate of the total emission of the vehicles in that group.

For the sake of simplicity, we suppose that all vehicles waiting in a queue will instantaneously react to the traffic light as it turns green, and there will be no delay for the following vehicles to imitate the speed of the leading vehicles. Therefore, for the vehicles that idle in front of a red light, after the light turns green the time-speed curves will overlap. Vehicles in each group will show the same combination of behaviors given in Section 3.1. For the representative vehicle, the time duration of each of these behaviors is considered to be the average of the time durations with that specific behavior for the first and the last vehicle in that group. For extracting the equations given in the following sections, the following lemma might be used, which is trivial to prove:

Lemma 3.1. *For a particle that starts moving with the initial speed "v_0" with a constant acceleration "a" the displacement, $\Delta x(t)$, after t time units is*

$$\Delta x(t) = \frac{1}{2}at^2 + v_0 t.$$

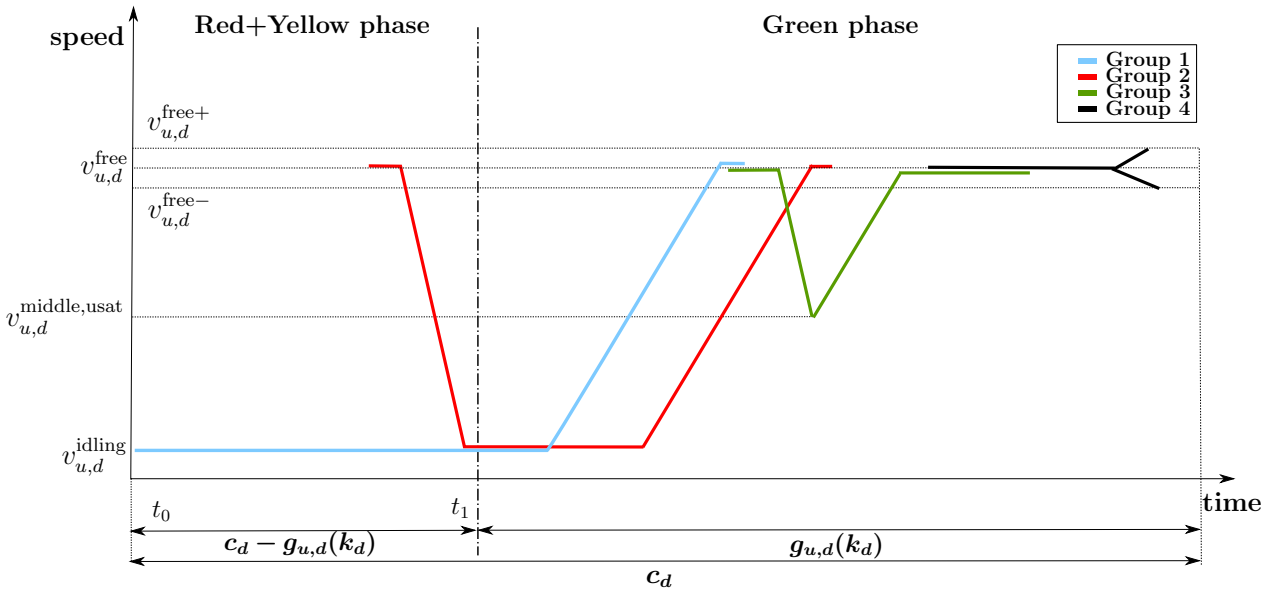

Figure 1: Traffic behaviors on link (u, d) within one cycle for the **under-saturated** urban traffic scenario

4 Flow-emission model for under-saturated scenario

The under-saturated scenario is observed when the demand (i.e., the number of vehicles waiting in the queue and the number of the arriving vehicles at the tail of the queue) is less than the number of vehicles that can be discharged by the saturated average leaving flow rate in one cycle. Hence, for the under-saturated scenario, the queue within the link will be completely dissolved during one cycle. Mathematically,

$$q_{u,d}(k_d) + c_d \cdot \alpha_{u,d}^{\text{arrive,q}}(k_d) \leq \sum_{o \in \mathcal{O}_{u,d}} \beta_{u,d,o} \cdot \mu_{u,d} \cdot g_{u,d,o}(k_d). \tag{11}$$

Suppose that each cycle starts by a red phase; then the vehicles observed within one cycle with an under-saturated condition are divided into the following four groups:

Group 1: composed of those vehicles that are already in the link standing in a queue at the beginning of the cycle (see the blue curve in Figure 1 for the average behavior of this group); they idle with a constant speed $v_{u,d}^{\text{idling}}$ from the beginning of the cycle till the traffic light turns green (at t_1 in Figure 1); then they accelerate[4] with $a_{u,d}^{\text{acc}}$ and move ahead till they leave the link. Looking at the average behavior of the representative vehicle of group 1 (the blue curve in Figure 1), the time instant at which the representative vehicle starts to accelerate is to the right of the instant t_1. This is because when the traffic light turns green, the vehicles in the queue can accelerate only one-by-one, i.e., the first vehicle in the queue starts to accelerate at t_1, while the other vehicles can accelerate only when the rest of the vehicles in the queue front of them have already accelerated (also see Figure 2(a), which represents the time-speed curve of the first and the last vehicle of group 1). As shown in Figure 1, this group of vehicles might also show a free-flow behavior at the end before they leave the link.

[4]For the sake of simplicity in the notations, for all the three scenarios under-saturated, saturated, and over-saturated, we have used the same acceleration $a_{u,d}^{\text{acc}}$ and deceleration $a_{u,d}^{\text{dec}}$. This can easily be extended by considering different acceleration rates $a_{u,d}^{\text{acc,usat}}$, $a_{u,d}^{\text{acc,sat}}$, and $a_{u,d}^{\text{acc,osat}}$, and different deceleration rates $a_{u,d}^{\text{dec,usat}}$, $a_{u,d}^{\text{dec,sat}}$, and $a_{u,d}^{\text{dec,osat}}$ for different traffic scenarios.

Group 2: composed of those vehicles that arrive at the tail of the waiting queue in the current cycle, after they decelerate from $v_{u,d}^{\text{free}}$ to $v_{u,d}^{\text{idling}}$. They idle for a while together with the waiting queue, and then start to accelerate as the traffic light turns green. The average behavior of this group is shown by the red time-speed curve in Figure 1.

Group 3: composed of those vehicles that arrive at the tail of the waiting queue in the current cycle, when the queue has already started to move. The representative of this group will decelerate with $a_{u,d}^{\text{dec}}$ to the speed $v_{u,d}^{\text{middle,usat}}$, which is larger than the idling speed. For $v_{u,d}^{\text{middle,usat}}$ we have

$$v_{u,d}^{\text{middle,usat}} = \frac{v_{u,d}^{\text{free}} + v_{u,d}^{\text{idling}}}{2}. \tag{12}$$

The green curve in Figure 1 shows the average behavior of this group. These vehicles might show a free-flow behavior at the end of their trip in the link.

Group 4: composed of those vehicles that arrive in the link with $v_{u,d}^{\text{free}}$, and continue moving ahead with this speed until they approach the end of the link and show a nonstop behavior (see the black curve in Figure 1 for the average behavior of this group).

We first give the formulas that represent the emission model corresponding to the urban under-saturated scenario. Then we explain in more detail how the time-speed curves and the following formulas are obtained. For the number of vehicles in each group, we have

$$n_{u,d}^{\text{G}_1,\text{usat}}(k_d) = q_{u,d}(k_d), \tag{13}$$

$$n_{u,d}^{\text{G}_2,\text{usat}}(k_d) = \alpha_{u,d}^{\text{arrive,q}}(k_d) \cdot T_{u,d}^{\text{arrive,G}_2,\text{usat}}(k_d), \tag{14}$$

$$n_{u,d}^{\text{G}_3,\text{usat}}(k_d) = \alpha_{u,d}^{\text{arrive,q}}(k_d) \cdot T_{u,d}^{\text{arrive,G}_3,\text{usat}}(k_d), \tag{15}$$

$$n_{u,d}^{\text{G}_4,\text{usat}}(k_d) = n_{u,d}^{\text{usat}}(k_d) - \sum_{i=1}^{3} n_{u,d}^{\text{G}_i,\text{usat}}(k_d), \tag{16}$$

with

$$T_{u,d}^{\text{arrive,G}_2,\text{usat}}(k_d) = \frac{\mu_{u,d}}{\mu_{u,d} - \alpha_{u,d}^{\text{arrive,q}}(k_d)} \left(c_d - g_{u,d}(k_d) + \frac{n_{u,d}^{\text{G}_1,\text{usat}}(k_d)}{\mu_{u,d}} - \tau_{u,d}^{\text{G}_2,\text{usat}}(k_d) \right), \tag{17}$$

$$T_{u,d}^{\text{arrive,G}_3,\text{usat}}(k_d) = \tau_{u,d}^{\text{G}_2,\text{usat}}(k_d) + \frac{v_{u,d}^{\text{free}} - v_{u,d}^{\text{idling}}}{a_{u,d}^{\text{acc}}}, \tag{18}$$

where $\tau_{u,d}^{\text{G}_2,\text{usat}}(k_d)$ is the average time duration that vehicles in group 2 take to reach the tail of the waiting queue in front of them from the time they enter the link. To compute $\tau_{u,d}^{\text{G}_2,\text{usat}}(k_d)$ within the time interval $[k_d c_d, (k_d+1)c_d)$, we assume that all vehicles will enter link (u,d) with $v_{u,d}^{\text{free}}$. If there are already some vehicles in front of them that are idling with $v_{u,d}^{\text{idling}}$ in a waiting queue, these vehicles should decelerate with $a_{u,d}^{\text{dec}}$ after a while in order to reach $v_{u,d}^{\text{idling}}$ as they approach the waiting queue. The total traveled distance by these vehicles until they reach the tail of the queue is $\frac{\left(C_{u,d} - q_{u,d}^{\text{ave}}(k_d)\right) l^{\text{veh}}}{N_{u,d}^{\text{lane}}}$ with $C_{u,d}$ the capacity of link (u,d), $q_{u,d}^{\text{ave}}(k_d)$ the average queue length on link (u,d) during

$[k_d c_d, (k_d+1)c_d)$, l^{veh} the average vehicle length, and $N^{\text{lane}}_{u,d}$ the number of lanes on link (u,d). Then from Lemma 3.1 we can write

$$\frac{\left(C_{u,d} - q^{\text{ave}}_{u,d}(k_d)\right) l^{\text{veh}}}{N^{\text{lane}}_{u,d}} = v^{\text{free}}_{u,d} \cdot T^{\text{free}}_{u,d}(k_d) + \frac{1}{2} a^{\text{dec}}_{u,d} \left(\frac{v^{\text{idling}}_{u,d} - v^{\text{free}}_{u,d}}{a^{\text{dec}}_{u,d}} \right)^2 + v^{\text{free}}_{u,d} \left(\frac{v^{\text{idling}}_{u,d} - v^{\text{free}}_{u,d}}{a^{\text{dec}}_{u,d}} \right), \tag{19}$$

which gives an expression for T^{free}. Knowing that

$$\tau^{\text{G}_2,\text{usat}}_{u,d}(k_d) = T^{\text{free}}_{u,d}(k_d) + \frac{v^{\text{idling}}_{u,d} - v^{\text{free}}_{u,d}}{a^{\text{dec}}_{u,d}}, \tag{20}$$

$\tau^{\text{G}_2,\text{usat}}_{u,d}(k_d)$ for $q^{\text{G}_2,\text{ave}}_{u,d}(k_d) = n^{\text{G}_1,\text{usat}}_{u,d}(k_d)$ is given by[5]

$$\tau^{\text{G}_2,\text{usat}}_{u,d}(k_d) = \frac{\left(C_{u,d} - n^{\text{G}_1,\text{usat}}_{u,d}(k_d)\right) l^{\text{veh}}}{N^{\text{lane}}_{u,d} v^{\text{free}}_{u,d}} - \frac{\left(v^{\text{idling}}_{u,d} - v^{\text{free}}_{u,d}\right)^2}{2 a^{\text{dec}}_{u,d} v^{\text{free}}_{u,d}}. \tag{21}$$

In order to compute the emissions for the under-saturated scenario, we need to find the number of the vehicles that show each of the driving behaviors "free", "idling", "decelerating", "accelerating", and "non-stop", and also the time duration of the free and idling behaviors during one cycle. Next, we will present these variables for the under-saturated urban traffic scenario.

- The number of vehicles in each of the groups 1-4 that show a free-flow behavior within one cycle is

$$\begin{aligned} n^{\text{free},\text{G}_1,\text{usat}}_{u,d}(k_d) &= n^{\text{G}_1,\text{usat}}_{u,d}(k_d), \\ n^{\text{free},\text{G}_2,\text{usat}}_{u,d}(k_d) &= n^{\text{G}_2,\text{usat}}_{u,d}(k_d), \\ n^{\text{free},\text{G}_3,\text{usat}}_{u,d}(k_d) &= n^{\text{G}_3,\text{usat}}_{u,d}(k_d), \\ n^{\text{free},\text{G}_4,\text{usat}}_{u,d}(k_d) &= n^{\text{G}_4,\text{usat}}_{u,d}(k_d), \end{aligned} \tag{22}$$

  and the average time duration that a vehicle in each of the groups spends showing the free-flow behavior is

$$\begin{aligned} T^{\text{free},\text{G}_1,\text{usat}}_{u,d}(k_d) &= \frac{\left(n^{\text{G}_1,\text{usat}}_{u,d}(k_d) + 0.5 n^{\text{G}_2,\text{usat}}_{u,d}(k_d)\right) l^{\text{veh}}}{N^{\text{lane}}_{u,d} v^{\text{free}}_{u,d}} - \frac{\left(v^{\text{free}}_{u,d}\right)^2 - \left(v^{\text{idling}}_{u,d}\right)^2}{2 a^{\text{acc}}_{u,d} v^{\text{free}}_{u,d}}, \\ T^{\text{free},\text{G}_2,\text{usat}}_{u,d}(k_d) &= \tau^{\text{G}_2,\text{usat}}_{u,d}(k_d) - \frac{v^{\text{idling}}_{u,d} - v^{\text{free}}_{u,d}}{a^{\text{dec}}_{u,d}} + T^{\text{free},\text{G}_1,\text{usat}}_{u,d}(k_d), \\ T^{\text{free},\text{G}_3,\text{usat}}_{u,d}(k_d) &= \frac{C_{u,d} l^{\text{veh}}}{N^{\text{lane}}_{u,d} v^{\text{free}}_{u,a}} + \left(v^{\text{free}}_{u,d} - v^{\text{idling}}_{u,d}\right) \frac{a^{\text{acc}}_{u,d} - a^{\text{dec}}_{u,d}}{2 a^{\text{dec}}_{u,d} a^{\text{acc}}_{u,d}}, \\ T^{\text{free},\text{G}_4,\text{usat}}_{u,d}(k_d) &= \frac{n^{\text{G}_4,\text{usat}}_{u,d}(k_d)}{\alpha^{\text{arrive,q}}_{u,d}(k_d)} - T^{\text{nonstop}}_{u,d}(k_d), \end{aligned} \tag{23}$$

  with

$$T^{\text{nonstop}}_{u,d}(k_d) = \begin{cases} \frac{v^{\text{free}+}_{u,d} - v^{\text{free}}_{u,d}}{a^{\text{acc}}_{u,d}}, & \text{if} \quad \frac{\alpha^{\text{arrive,q}}_{u,d}(k)}{\mu_{u,d}} \le \lambda_{u,d}, \\ \frac{v^{\text{free}}_{u,d} - v^{\text{free}-}_{u,d}}{a^{\text{dec}}_{u,d}}, & \text{if} \quad \frac{\alpha^{\text{arrive,q}}_{u,d}(k)}{\mu_{u,d}} > \lambda_{u,d}, \end{cases} \tag{24}$$

  and $\lambda_{u,d}$ defined in Section 3.1 as a threshold in $[0,1]$ found based on historical traffic data for detecting a heavy and light traffic condition in a link.

[5]Note that based on the definitions given above for different groups of vehicles, the queue in front of the vehicles in group 2 is formed by the vehicles in group 1 (also see Figure 1).

- The number of vehicles that show an idling behavior within one cycle is

$$\begin{aligned} n_{u,d}^{\text{idling,G}_1,\text{usat}}(k_d) &= n_{u,d}^{\text{G}_1,\text{usat}}(k_d), \\ n_{u,d}^{\text{idling,G}_2,\text{usat}}(k_d) &= n_{u,d}^{\text{G}_2,\text{usat}}(k_d), \\ n_{u,d}^{\text{idling,G}_3,\text{usat}}(k_d) &= 0, \\ n_{u,d}^{\text{idling,G}_4,\text{usat}}(k_d) &= 0, \end{aligned} \tag{25}$$

and the average time duration that a vehicle in each of the groups spends showing the idling behavior is

$$\begin{aligned} T_{u,d}^{\text{idling,G}_1,\text{usat}}(k_d) &= c_d - g_{u,d}(k_d) + \frac{n_{u,d}^{\text{G}_1,\text{usat}}(k_d)}{2\mu_{u,d}}, \\ T_{u,d}^{\text{idling,G}_2,\text{usat}}(k_d) &= T_{u,d}^{\text{idling,G}_1,\text{usat}}(k_d) - \tau_{u,d}^{\text{G}_2,\text{usat}}(k_d), \\ T_{u,d}^{\text{idling,G}_3,\text{usat}}(k_d) &= 0, \\ T_{u,d}^{\text{idling,G}_4,\text{usat}}(k_d) &= 0. \end{aligned} \tag{26}$$

- The number of vehicles that show a decelerating behavior within one cycle is

$$\begin{aligned} n_{u,d}^{\text{dec,G}_1,\text{usat}}(k_d) &= 0, \\ n_{u,d}^{\text{dec,G}_2,\text{usat}}(k_d) &= n_{u,d}^{\text{G}_2,\text{usat}}(k_d), \\ n_{u,d}^{\text{dec,G}_3,\text{usat}}(k_d) &= n_{u,d}^{\text{G}_3,\text{usat}}(k_d), \\ n_{u,d}^{\text{dec,G}_4,\text{usat}}(k_d) &= \begin{cases} 0, & \text{for light traffic,} \\ n_{u,d}^{\text{G}_4,\text{usat}}(k_d), & \text{for heavy traffic,} \end{cases} \end{aligned} \tag{27}$$

and the average time duration that a vehicle spends showing the decelerating behavior is

$$\begin{aligned} T_{u,d}^{\text{dec,G}_1,\text{usat}}(k_d) &= 0, \\ T_{u,d}^{\text{dec,G}_2,\text{usat}}(k_d) &= \frac{v_{u,d}^{\text{idling}} - v_{u,d}^{\text{free}}}{a_{u,d}^{\text{dec}}}, \\ T_{u,d}^{\text{dec,G}_3,\text{usat}}(k_d) &= \frac{v_{u,d}^{\text{middle,usat}} - v_{u,d}^{\text{free}}}{a_{u,d}^{\text{dec}}}, \\ T_{u,d}^{\text{dec,G}_4,\text{usat}}(k_d) &= \begin{cases} 0, & \text{for light traffic,} \\ \frac{v_{u,d}^{\text{free}-} - v_{u,d}^{\text{free}}}{a_{u,d}^{\text{dec}}}, & \text{for heavy traffic.} \end{cases} \end{aligned} \tag{28}$$

- The number of vehicles that show an accelerating behavior within one cycle is

$$\begin{aligned} n_{u,d}^{\text{acc,G}_1,\text{usat}}(k_d) &= n_{u,d}^{\text{G}_2,\text{usat}}(k_d), \\ n_{u,d}^{\text{acc,G}_2,\text{usat}}(k_d) &= n_{u,d}^{\text{G}_2,\text{usat}}(k_d), \\ n_{u,d}^{\text{acc,G}_3,\text{usat}}(k_d) &= n_{u,d}^{\text{G}_3,\text{usat}}(k_d), \\ n_{u,d}^{\text{acc,G}_4,\text{usat}}(k_d) &= \begin{cases} n_{u,d}^{\text{G}_4,\text{usat}}(k_d), & \text{for light traffic,} \\ 0, & \text{for heavy traffic,} \end{cases} \end{aligned} \tag{29}$$

and the average time duration that a vehicle spends showing the accelerating behavior is

$$\begin{aligned} T_{u,d}^{\text{acc,G}_1,\text{usat}}(k_d) &= \frac{v_{u,d}^{\text{free}} - v_{u,d}^{\text{idling}}}{a_{u,d}^{\text{acc}}}, \\ T_{u,d}^{\text{acc,G}_2,\text{usat}}(k_d) &= \frac{v_{u,d}^{\text{free}} - v_{u,d}^{\text{idling}}}{a_{u,d}^{\text{acc}}}, \\ T_{u,d}^{\text{acc,G}_3,\text{usat}}(k_d) &= \frac{v_{u,d}^{\text{free}} - v_{u,d}^{\text{middle,usat}}}{a_{u,d}^{\text{acc}}}, \\ T_{u,d}^{\text{acc,G}_4,\text{usat}}(k_d) &= \begin{cases} \frac{v_{u,d}^{\text{free}+} - v_{u,d}^{\text{free}}}{a_{u,d}^{\text{acc}}}, & \text{for light traffic,} \\ 0, & \text{for heavy traffic.} \end{cases} \end{aligned} \tag{30}$$

Here we explain in more detail how the time-speed curves represented in Figure 1 and correspondingly the given equations for the under-saturated scenario are obtained. Since for the under-saturated scenario all vehicles that are initially waiting in the queue will have enough time to leave the link within one cycle, we consider them as one group, and illustrate the behavior of the representative of this group (shown in blue in Figure 1) as the average of the time-speed curves of the first and the last vehicle in the group.

In Figure 2(a), the time-speed curves of the first, the last, and the representative vehicle in group 1 are shown. The blue (solid) curve in this figure, which demonstrates the behavior of the representative vehicle, is the same as the blue curve in Figure 1. The first vehicle of group 1 will immediately start to accelerate as the traffic light turns green at t_1 (see Figure 2(a)). After its speed reaches $v_{u,d}^{\text{free}}$, this vehicle might move with $v_{u,d}^{\text{free}}$ (depending on the length of the link, the free-flow speed, the acceleration, etc.) for a while before it leaves the link. The last vehicle of group 1 will start to accelerate only after all other vehicles in group 1 have done so.

Since for the under-saturated scenario, the leaving rate of the vehicles in the queue is the saturated leaving flow rate (i.e., $\mu_{u,d}$), we can write

$$t_{\text{last}}^{\text{acc},\text{G}_1,\text{usat}}(k_d) - t_{\text{first}}^{\text{acc},\text{G}_1,\text{usat}}(k_d) = \frac{n_{u,d}^{\text{G}_1,\text{usat}}(k_d)}{\mu_{u,d}}, \tag{31}$$

where $t_{\text{first}}^{\text{acc,usat,G}_1}(k_d)$ and $t_{\text{last}}^{\text{acc,usat,}G_1}(k_d)$ denote, respectively, the time instant the first and the last vehicle in group 1 start to accelerate. Hence, the idling times of the first and the last vehicle in group 1 are

$$T_{\text{first}}^{\text{idling},\text{G}_1,\text{usat}}(k_d) = c_d - g_{u,d}(k_d), \tag{32}$$

$$T_{\text{last}}^{\text{idling},\text{G}_1,\text{usat}}(k_d) = c_d - g_{u,d}(k_d) + \frac{n_{u,d}^{\text{G}_1,\text{usat}}(k_d)}{\mu_{u,d}}. \tag{33}$$

The idling time of the representative vehicle of group 1 for the under-saturated scenario is the average of the idling times of the first and the last vehicle (see the first equation of (26)), i.e.,

$$T_{\text{rep}}^{\text{idling},\text{G}_1,\text{usat}}(k_d) = c_d - g_{u,d}(k_d) + \frac{n_{u,d}^{\text{G}_1,\text{usat}}(k_d)}{2\mu_{u,d}}. \tag{34}$$

Figure 2(b) illustrates the time-speed curves of the first, the last, and the representative vehicle in group 2 of the under-saturated scenario, where the red curve (corresponding to the representative vehicle of group 2) is identical with the red (solid) curve in Figure 1. Similar to the vehicles in group 1, a free-flow behavior might or might not be observed at the end of the trip for vehicles in group 2. After the traffic light turns green, vehicles in group 2 will start to accelerate with a delay; the first vehicle will accelerate just after the last vehicle in group 1 does (i.e., at $t_{\text{last}}^{\text{acc},\text{G}_1,\text{usat}}(k_d)$ in Figure 2(a), which is the same as $t_{\text{first}}^{\text{acc},\text{G}_2,\text{usat}}(k_d)$ in Figure 2(b)). The last vehicle of group 2 will move ahead such that it starts to accelerate immediately after it reaches $v_{u,d}^{\text{idling}}$ (see Figure 2(b)). Note that since the next arriving vehicle decelerates to a speed higher than $v_{u,d}^{\text{idling}}$ (i.e., it does not idle at all), it will be put in a separate group, i.e., group 3 discussed later.

All vehicles in group 2 become a part of the waiting queue before they start to accelerate, and they will also leave the link with rate $\mu_{u,d}$. The total travel time of the first vehicle in group 2 is composed of the following terms:

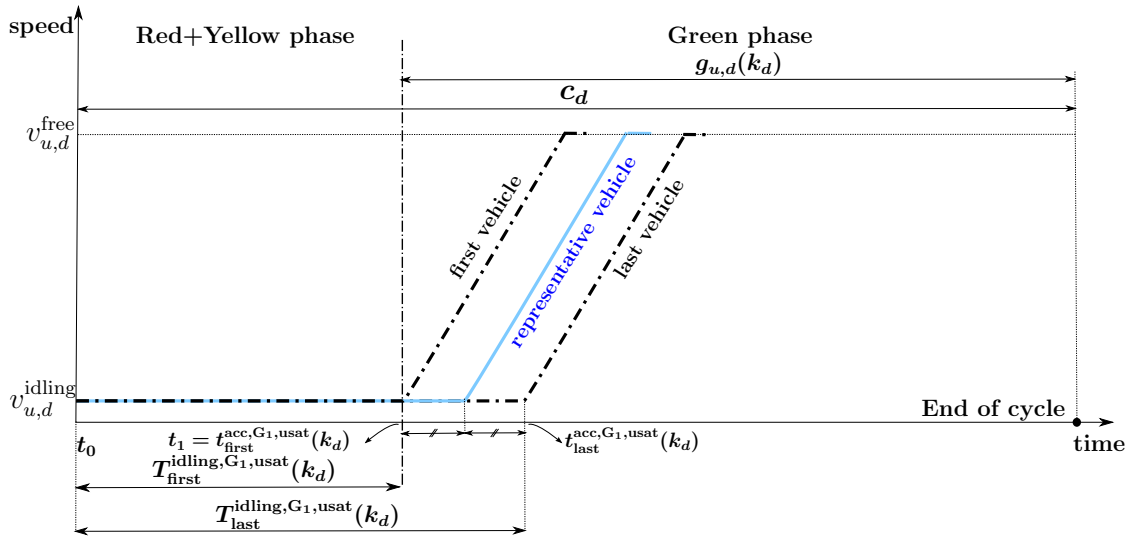

(a) Traffic behaviors for the first, last, and representative vehicle in group 1

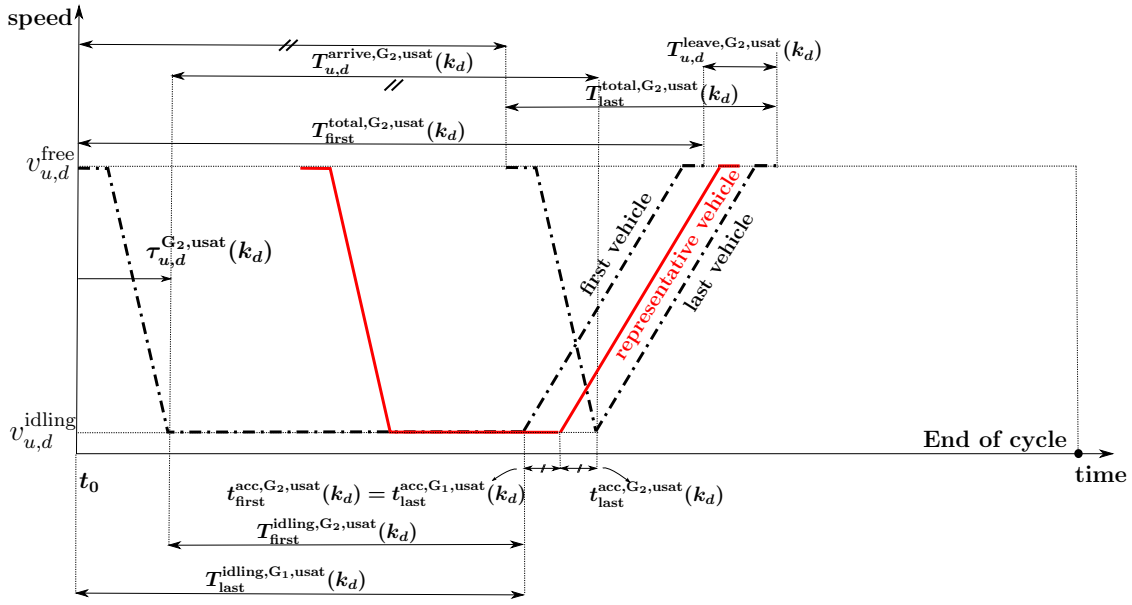

(b) Traffic behaviors for the first, last, and representative vehicle in group 2

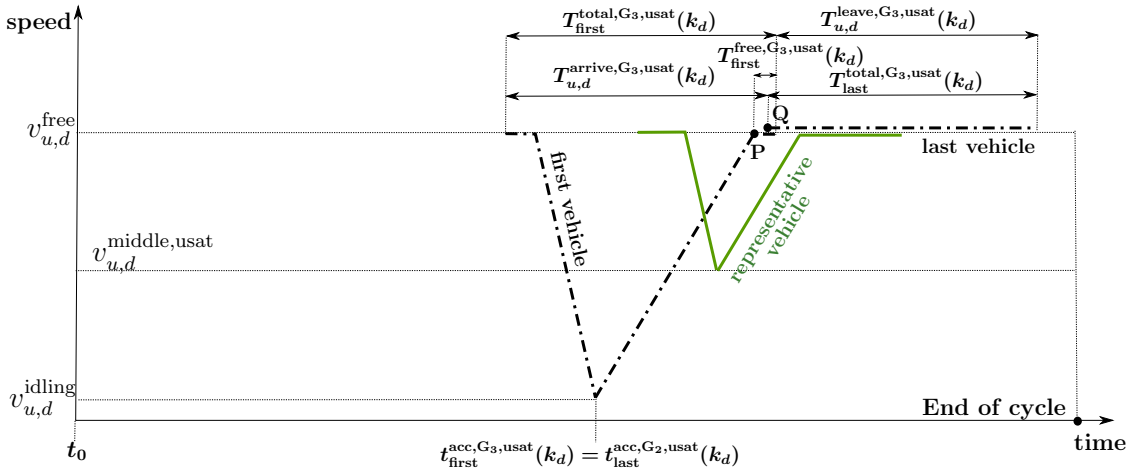

(c) Traffic behaviors for the first, last, and representative vehicle in group 3

Figure 2: Traffic behavior of different groups for **under-saturated** urban traffic scenario

- free-flow (start) + decelerating:

$$\tau_{u,d}^{\mathrm{G}_2,\mathrm{usat}}(k_d), \tag{35}$$

where $\tau_{u,d}^{\mathrm{G}_2,\mathrm{usat}}(k_d)$ is the average time duration for the vehicles in group 2 to reach the tail of the waiting queue from the instant they enter the link (see Figure 2(b)). Note that the time period of the free-flow behavior (at start) alone is

$$\tau_{u,d}^{\mathrm{G}_2,\mathrm{usat}}(k_d) - \frac{v_{u,d}^{\mathrm{idling}} - v_{u,d}^{\mathrm{free}}}{a_{u,d}^{\mathrm{dec}}}; \tag{36}$$

- idling (see Figure 2(b)):

$$T_{\mathrm{last}}^{\mathrm{idling},\mathrm{G}_1,\mathrm{usat}}(k_d) - \tau_{u,d}^{\mathrm{G}_2,\mathrm{usat}}(k_d); \tag{37}$$

- accelerating:

$$\frac{v_{u,d}^{\mathrm{free}} - v_{u,d}^{\mathrm{idling}}}{a_{u,d}^{\mathrm{acc}}}; \tag{38}$$

- free-flow (end):

$$\frac{n_{u,d}^{\mathrm{G}_1,\mathrm{usat}}(k_d) l^{\mathrm{veh}}}{N_{u,d}^{\mathrm{lane}} v_{u,d}^{\mathrm{free}}} - \frac{\left(v_{u,d}^{\mathrm{free}}\right)^2 - \left(v_{u,d}^{\mathrm{idling}}\right)^2}{2a_{u,d}^{\mathrm{acc}} v_{u,d}^{\mathrm{free}}}. \tag{39}$$

We should notice that the number of the vehicles in front of the first vehicle in group 2 is $n_{u,d}^{\mathrm{G}_1,\mathrm{usat}}(k_d)$ when the traffic light turns green. This means that a distance of $\frac{n_{u,d}^{\mathrm{G}_1,\mathrm{usat}}(k_d) l^{\mathrm{veh}}}{N_{u,d}^{\mathrm{lane}}}$ should be traveled by the first vehicle of this group to cross the traffic light (partly by the constant acceleration $a_{u,d}^{\mathrm{acc}}$ and partly by the constant speed $v_{u,d}^{\mathrm{free}}$). From Lemma 3.1, we obtain

$$\frac{n_{u,d}^{\mathrm{G}_1,\mathrm{sat}}(k_d) l^{\mathrm{veh}}}{N_{u,d}^{\mathrm{lane}}} = v_{u,d}^{\mathrm{free}} \cdot T_{\mathrm{first}}^{\mathrm{free}} + \frac{a_{u,d}^{\mathrm{acc}}}{2}\left(\frac{v_{u,d}^{\mathrm{free}} - v_{u,d}^{\mathrm{idling}}}{a_{u,d}^{\mathrm{acc}}}\right)^2 + v_{u,d}^{\mathrm{idling}}\left(\frac{v_{u,d}^{\mathrm{free}} - v_{u,d}^{\mathrm{idling}}}{a_{u,d}^{\mathrm{acc}}}\right), \tag{40}$$

which reduces to (39).

Similarly, we can find the total travel time of the last vehicle of group 2, which is the same as for the first vehicle (resulting in the second equations of (26), (28), and (30)) except that it does not include the idling time, and that the free-flow (end) time duration using Lemma 3.1 is[6]

$$\frac{\left(n_{u,d}^{\mathrm{G}_1,\mathrm{usat}}(k_d) + n_{u,d}^{\mathrm{G}_2,\mathrm{usat}}(k_d)\right) l^{\mathrm{veh}}}{N_{u,d}^{\mathrm{lane}} v_{u,d}^{\mathrm{free}}} - \frac{\left(v_{u,d}^{\mathrm{free}}\right)^2 - \left(v_{u,d}^{\mathrm{idling}}\right)^2}{2a_{u,d}^{\mathrm{acc}} v_{u,d}^{\mathrm{free}}}. \tag{41}$$

Therefore, for the representative vehicle of group 2, the time duration of the free-flow behavior at the end of its presence in the link (see the first two equations of (23)) is:

$$\frac{\left(n_{u,d}^{\mathrm{G}_1,\mathrm{usat}}(k_d) + 0.5 n_{u,d}^{\mathrm{G}_2,\mathrm{usat}}(k_d)\right) l^{\mathrm{veh}}}{N_{u,d}^{\mathrm{lane}} v_{u,d}^{\mathrm{free}}} - \frac{\left(v_{u,d}^{\mathrm{free}}\right)^2 - \left(v_{u,d}^{\mathrm{idling}}\right)^2}{2a_{u,d}^{\mathrm{acc}} v_{u,d}^{\mathrm{free}}}. \tag{42}$$

[6]Note that the number of the vehicles in front of the last vehicle in group 2 is $n_{u,d}^{\mathrm{G}_1,\mathrm{usat}}(k_d) + n_{u,d}^{\mathrm{G}_2,\mathrm{usat}}(k_d)$

Note that for the sake of simplicity, we assume that the average time duration of the free-flow behavior at the end of the trip for the vehicles in group 1 and 2 are the same (see the first two equations of (23)).

Finally, for the vehicles in group 2 we can write

$$\alpha_{u,d}^{\text{arrive,q}}(k_d)T_{u,d}^{\text{arrive,G}_2,\text{usat}}(k_d) = \mu_{u,d}T_{u,d}^{\text{leave,G}_2,\text{usat}}(k_d), \tag{43}$$

where $T_{u,d}^{\text{arrive,G}_2,\text{usat}}(k_d)$ is the time duration during which vehicles in group 2 reach the tail of the queue, and $T_{u,d}^{\text{leave,G}_2,\text{usat}}(k_d)$ is the time duration during which vehicles in group 2 leave the link. Moreover, from Figure 2(b) we have

$$T_{u,d}^{\text{arrive,G}_2,\text{usat}}(k_d) + T_{\text{last}}^{\text{total,G}_2,\text{usat}}(k_d) = T_{u,d}^{\text{leave,G}_2,\text{usat}}(k_d) + T_{\text{first}}^{\text{total,G}_2,\text{usat}}(k_d), \tag{44}$$

which results in (17) given in Section 4. Note that from (11), $\alpha_{u,d}^{\text{arrive,q}}(k_d) < \mu_{u,d}$, and hence the denominator of (17) will never become zero.

The second group of the arriving vehicles are put in group 3 of the under-saturated scenario. They are different from vehicles in group 2 in the sense that they will also decelerate, but to speed values larger than $v_{u,d}^{\text{idling}}$ (since the queue composed of groups 1 and 2 has already started to move and there is no need anymore for the arriving vehicles to idle). Figure 2(c) shows the time-speed curves of the first, the last, and the representative vehicle in group 3. Comparing this figure with Figure 1, the green curves, i.e., the time-speed curves of the representative vehicle in group 3, are the same.

The first vehicle in group 3 arrives just after the last vehicle in group 2 (see Figure 2(c)). In the limit, the time-speed curves of the last vehicle in group 2 and the first vehicle in group 3 become exactly the same (compare Figures 2(b) and 2(c)). The next arriving vehicles will show the same behavior as the first vehicle, but each of them decelerates to a speed (we call it the *transition speed*) that is in general larger than the speed of the previous vehicle (i.e., the transition speed increases gradually for successive vehicles). The time-speed curve corresponding to the last vehicle in group 3 becomes a straight line in the limit (see Figure 2(c)). Note that point "P" in this figure separates groups 3 and 4 w.r.t. the arrival times. Point "Q" is the starting point of the time-speed curve of the last vehicle in group 3. The transition speed corresponding to the representative vehicle in group 3, i.e., the middle speed $v_{u,d}^{\text{middle,usat}}$ is the mean value of the transition speed of the first vehicles (i.e., $v_{u,d}^{\text{idling}}$) and the last vehicle (i.e., $v_{u,d}^{\text{free}}$). Therefore, we obtain (12).

Moreover, since the vehicles in group 3 will not idle at all during the entire cycle, the leaving flow rate for them is the same as their arriving flow rate, i.e.,

$$\alpha_{u,d}^{\text{leave,l,G}_3}(k_d) = \alpha_{u,d}^{\text{arrive,l,G}_3}(k_d). \tag{45}$$

From Figure 2(c), we can write

$$\alpha_{u,d}^{\text{arrive,q}}(k_d)T_{u,d}^{\text{arrive,G}_3,\text{usat}}(k_d) = \alpha_{u,d}^{\text{leave,l}}(k_d)T_{u,d}^{\text{leave,G}_3,\text{usat}}(k_d), \tag{46}$$

which in combination with (45) gives

$$T_{u,d}^{\text{arrive,G}_3,\text{usat}}(k_d) = T_{u,d}^{\text{leave,G}_3,\text{usat}}(k_d), \tag{47}$$

In addition, from (47) and Figure 2(c), we obtain

$$T_{\text{last}}^{\text{total,G}_3,\text{usat}}(k_d) = T_{\text{first}}^{\text{total,G}_3,\text{usat}}(k_d). \tag{48}$$

The last vehicle in group 3 travels through the entire link with a constant speed of $v_{u,d}^{\text{free}}$. Hence,

$$T_{\text{last}}^{\text{G}_3,\text{usat}}(k_d) = \frac{C_{u,d} l^{\text{veh}}}{N_{u,d}^{\text{lane}} v_{u,d}^{\text{free}}}, \tag{49}$$

where $\frac{C_{u,d} l^{\text{veh}}}{N_{u,d}^{\text{lane}}}$ is the total length of the link. For the first vehicle in group 3 we have:

$$T_{\text{first}}^{\text{total},\text{G}_3,\text{usat}}(k_d) = \frac{v_{u,d}^{\text{idling}} - v_{u,d}^{\text{free}}}{a_{u,d}^{\text{dec}}} + \frac{v_{u,d}^{\text{free}} - v_{u,d}^{\text{idling}}}{a_{u,d}^{\text{acc}}} + T_{\text{first}}^{\text{free},\text{G}_3,\text{usat}}(k_d), \tag{50}$$

and from (48) and (49), we finally have

$$T_{\text{first}}^{\text{free},\text{G}_3,\text{usat}}(k_d) = \frac{C_{u,d} l^{\text{veh}}}{N_{u,d}^{\text{lane}} v_{u,d}^{\text{free}}} - \frac{v_{u,d}^{\text{idling}} - v_{u,d}^{\text{free}}}{a_{u,d}^{\text{dec}}} - \frac{v_{u,d}^{\text{free}} - v_{u,d}^{\text{idling}}}{a_{u,d}^{\text{acc}}}, \tag{51}$$

which is indeed the third equation of (23). Assuming that $\alpha_{u,d}^{\text{arrive,q}}(k_d)$ is large enough, points P and Q will coincide. Therefore, (18) will be obtained.

The rest of the equations of the under-saturated model that are not explained in detail explicitly can easily be obtained with a similar approach (also see Figure 1).

5 Flow-emission model for saturated scenario

The saturated scenario is observed when the demand is larger than the number of vehicles that can be discharged by the saturated average leaving flow rate in one cycle. For the saturated traffic scenario, the initial queue in the link will completely be dissolved during one cycle, but a new queue will be formed by a part of the arriving vehicles (i.e., not all the arriving vehicles in a saturated traffic scenario can leave the link during the green phase). Mathematically,

$$q_{u,d}(k_d) \leq \sum_{o \in \mathcal{O}_{u,d}} \beta_{u,d,o} \cdot \mu_{u,d} \cdot g_{u,d,o}(k_d) < q_{u,d}(k_d) + c_d \cdot \alpha_{u,d}^{\text{arrive,q}}(k_d). \tag{52}$$

For a saturated urban traffic scenario, the average leaving flow rate during the entire cycle is the saturated leaving flow rate, $\mu_{u,d}$. Two cases are possible, i.e., $\alpha_{u,d}^{\text{arrive,q}}(k_d) < \mu_{u,d}$ and $\alpha_{u,d}^{\text{arrive,q}}(k_d) \geq \mu_{u,d}$, which result in different model equations. We first develop the model for case 1, i.e., $\alpha_{u,d}^{\text{arrive,q}}(k_d) < \mu_{u,d}$, and later we extend the model for case 2, i.e., $\alpha_{u,d}^{\text{arrive,q}}(k_d) \geq \mu_{u,d}$.

5.1 Case 1: $\alpha_{u,d}^{\text{arrive,q}}(k_d) < \mu_{u,d}$

For the sake of simplicity, we avoid to repeat "case 1" in this section. First, we give the equations, and then we explain how the equations are obtained. Some of the equations may not be explained explicitly, as they can be easily found with a similar approach as for the under-saturated scenario considering Figure 4. The vehicles observed during one cycle are divided into the following three groups:

Group 1: composed of those vehicles that are already in the link standing in a queue at the beginning of the cycle (see the blue curve in Figure 3 for the average behavior of this group); the average behavior of this group is identical to that of the first group for an under-saturated scenario (see Section 4).

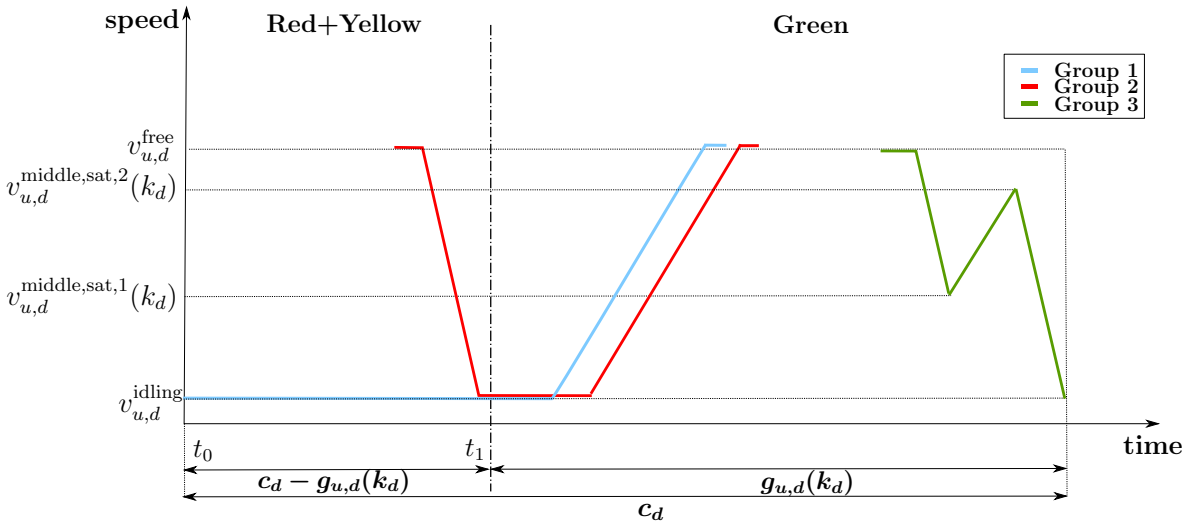

Figure 3: Traffic behaviors on link (u, d) within one cycle for the **saturated** urban traffic scenario, case 1: $\alpha_{u,d}^{\text{arrive,q}}(k_d) < \mu_{u,d}$

Group 2: composed of those vehicles that arrive at the tail of the waiting queue during the current cycle after they decelerate from $v_{u,d}^{\text{free}}$ to $v_{u,d}^{\text{idling}}$. They idle for a while behind the initial queue, and then accelerate just after the queue in front of them has been dissolved. They finally leave the link during the current cycle (see the red curve in Figure 3 for the average behavior of this group). The observed behavior for this group of vehicles, is the same as the observed behavior for group 2 in the under-saturated scenario.

Group 3: composed of those vehicles that arrive at the tail of the queue in the current cycle, when the queue in front of them has already started to move. Therefore, they should first decelerate from $v_{u,d}^{\text{free}}$ to a speed value larger than $v_{u,d}^{\text{idling}}$, i.e., to $v_{u,d}^{\text{middle,sat,1}}(k_d)$ (see the green curve in Figure 3 for the average behavior of this group). Then, with the moving traffic they also accelerate to reach the speed $v_{u,d}^{\text{middle,sat,2}}(k_d)$, when they notice that there is not enough time to reach and pass the traffic light, and they decelerate again to reach $v_{u,d}^{\text{idling}}$ by the time the traffic light turns red. The values of $v_{u,d}^{\text{middle,sat,1}}(k_d)$ and $v_{u,d}^{\text{middle,sat,2}}$ are computed by

$$v_{u,d}^{\text{middle,sat,1}}(k_d) = \frac{v_{u,d}^{\text{idling}} + v_{u,d}^{\text{middle,sat,2}}(k_d)}{2}, \tag{53}$$

$$v_{u,d}^{\text{middle,sat,2}}(k_d) = v_{u,d}^{\text{idling}} + \frac{n_{u,d}^{\text{G}_3,\text{sat}}(k_d)}{\alpha_{u,d}^{\text{arrive,q}}(k_d)} \cdot \frac{a_{u,d}^{\text{acc}} a_{u,d}^{\text{dec}}}{a_{u,d}^{\text{dec}} - a_{u,d}^{\text{acc}}}. \tag{54}$$

For the number of vehicles in each of the groups, we have

$$n_{u,d}^{\mathrm{G}_1,\mathrm{sat}}(k_d) = q_{u,d}(k_d), \tag{55}$$

$$n_{u,d}^{\mathrm{G}_2,\mathrm{sat}}(k_d) = \min\left\{ n_{u,d}^{\mathrm{sat}}(k_d) - n_{u,d}^{\mathrm{G}_1,\mathrm{sat}}(k_d), \max\left\{ \alpha_{u,d}^{\mathrm{arrive,q}}(k_d)\cdot T_{u,d}^{\mathrm{arrive,G_2,sat}}(k_d), \right.\right.$$
$$\left.\left. n_{u,d}^{\mathrm{sat}}(k_d) - n_{u,d}^{\mathrm{G}_1,\mathrm{sat}}(k_d) - \alpha_{u,d}^{\mathrm{arrive,q}}(k_d)\left(v_{u,d}^{\mathrm{free}} - v_{u,d}^{\mathrm{idling}}\right)\left(\frac{1}{a_{u,d}^{\mathrm{acc}}} - \frac{1}{a_{u,d}^{\mathrm{dec}}}\right)\right\}\right\}, \tag{56}$$

$$n_{u,d}^{\mathrm{G}_3,\mathrm{sat}}(k_d) = n_{u,d}^{\mathrm{sat}}(k_d) - \sum_{i=1}^{2} n_{u,d}^{\mathrm{G}_i,\mathrm{sat}}(k_d), \tag{57}$$

with $T_{u,d}^{\mathrm{arrive,G_2,sat}}(k_d)$ computed by

$$T_{u,d}^{\mathrm{arrive,G_2,sat}}(k_d) = \frac{N_{u,d}^{\mathrm{lane}} v_{u,d}^{\mathrm{free}}}{N_{u,d}^{\mathrm{lane}} v_{u,d}^{\mathrm{free}} + \alpha_{u,d}^{\mathrm{arrive,q}}(k_d) l^{\mathrm{veh}}} \cdot \left(c_d - \frac{n_{u,d}^{\mathrm{G}_1,\mathrm{sat}}(k_d) l^{\mathrm{veh}}}{N_{u,d}^{\mathrm{lane}} v_{u,d}^{\mathrm{free}}} + \frac{\left(v_{u,d}^{\mathrm{free}}\right)^2 - \left(v_{u,d}^{\mathrm{idling}}\right)^2}{2 v_{u,d}^{\mathrm{free}} a_{u,d}^{\mathrm{acc}}} - \tau_{u,d}^{\mathrm{G_2,sat}}(k_d) \right), \tag{58}$$

and $\tau_{u,d}^{\mathrm{G_2,sat}}(k_d)$ computed similarly to $\tau_{u,d}^{\mathrm{G_2,usat}}(k_d)$ by (21).

The number of vehicles in each group that show a specific behavior, and also the time duration that each vehicle shows the behavior are given next. These values can be used to compute the emissions in the saturated scenario using the equations introduced in Section 3.2.

- For the free-flow behavior, we have

$$\begin{aligned} n_{u,d}^{\mathrm{free,G_1,sat}}(k_d) &= n_{u,d}^{\mathrm{G_1,sat}}(k_d), \\ n_{u,d}^{\mathrm{free,G_2,sat}}(k_d) &= n_{u,d}^{\mathrm{G_2,sat}}(k_d), \\ n_{u,d}^{\mathrm{free,G_3,sat}}(k_d) &= n_{u,d}^{\mathrm{G_3,sat}}(k_d), \end{aligned} \tag{59}$$

  and

$$\begin{aligned} T_{u,d}^{\mathrm{free,G_1,sat}}(k_d) &= \frac{\left(n_{u,d}^{\mathrm{G_1,sat}}(k_d) + 0.5 n_{u,d}^{\mathrm{G_2,sat}}(k_d)\right) l^{\mathrm{veh}}}{v_{u,d}^{\mathrm{free}}} - \frac{\left(v_{u,d}^{\mathrm{free}}\right)^2 - \left(v_{u,d}^{\mathrm{idling}}\right)^2}{2 a_{u,d}^{\mathrm{acc}} v_{u,d}^{\mathrm{free}}}, \\ T_{u,d}^{\mathrm{free,G_2,sat}}(k_d) &= \tau_{u,d}^{\mathrm{G_2,sat}}(k_d) - \frac{v_{u,d}^{\mathrm{idling}} - v_{u,d}^{\mathrm{free}}}{a_{u,d}^{\mathrm{dec}}} + T_{u,d}^{\mathrm{free,G_1,sat}}(k_d), \\ T_{u,d}^{\mathrm{free,G_3,sat}}(k_d) &= \tau_{u,d}^{\mathrm{G_3,sat}}(k_d) - \frac{v_{u,d}^{\mathrm{middle,sat,1}}(k_d) - v_{u,d}^{\mathrm{free}}}{a_{u,d}^{\mathrm{dec}}}, \end{aligned} \tag{60}$$

  with $\tau_{u,d}^{\mathrm{G_3,sat}}(k_d)$ computed by[7]

$$\tau_{u,d}^{\mathrm{G_3,sat}}(k_d) = \frac{C_{u,d} - n_{u,d}^{\mathrm{G_1,usat}}(k_d) - n_{u,d}^{\mathrm{G_2,usat}}(k_d)}{N_{u,d}^{\mathrm{lane}} v_{u,d}^{\mathrm{free}}} l^{\mathrm{veh}} - \frac{\left(v_{u,d}^{\mathrm{middle,sat,1}}(k_d) - v_{u,d}^{\mathrm{free}}\right)^2}{2 a_{u,d}^{\mathrm{dec}} v_{u,d}^{\mathrm{free}}}. \tag{61}$$

[7]Note that the number of vehicles already in the queue in front of group 3 is $n_{u,d}^{\mathrm{G_1,usat}}(k_d) + n_{u,d}^{\mathrm{G_2,usat}}(k_d)$, and the queue is already moving forward with $v_{u,d}^{\mathrm{middle,sat,1}}(k_d)$.

- For the idling behavior, we have

$$\begin{aligned} n_{u,d}^{\text{idling,G}_1,\text{sat}}(k_d) &= n_{u,d}^{\text{G}_1,\text{sat}}(k_d), \\ n_{u,d}^{\text{idling,G}_2,\text{sat}}(k_d) &= n_{u,d}^{\text{G}_2,\text{sat}}(k_d), \\ n_{u,d}^{\text{idling,G}_3,\text{sat}}(k_d) &= 0, \end{aligned} \tag{62}$$

and

$$\begin{aligned} T_{u,d}^{\text{idling,G}_1,\text{sat}}(k_d) &= c_d - g_{u,d}(k_d) + \frac{0.5 n_{u,d}^{\text{G}_1,\text{sat}}(k_d)}{\mu_{u,d}}, \\ T_{u,d}^{\text{idling,G}_2,\text{sat}}(k_d) &= T_{u,d}^{\text{idling,G}_1,\text{sat}}(k_d) - \tau_{u,d}^{\text{G}_2,\text{sat}}(k_d), \\ T_{u,d}^{\text{idling,G}_3,\text{sat}}(k_d) &= 0. \end{aligned} \tag{63}$$

- For the decelerating behavior, we have

$$\begin{aligned} n_{u,d}^{\text{dec,G}_1,\text{sat}}(k_d) &= 0, \\ n_{u,d}^{\text{dec,G}_2,\text{sat}}(k_d) &= n_{u,d}^{\text{G}_2,\text{sat}}(k_d), \\ n_{u,d}^{\text{dec,G}_3,\text{sat}}(k_d) &= n_{u,d}^{\text{G}_3,\text{sat}}(k_d), \end{aligned} \tag{64}$$

and

$$\begin{aligned} T_{u,d}^{\text{dec,G}_1,\text{sat}}(k_d) &= 0, \\ T_{u,d}^{\text{dec,G}_2,\text{sat}}(k_d) &= \frac{v_{u,d}^{\text{idling}} - v_{u,d}^{\text{free}}}{a_{u,d}^{\text{dec}}}, \\ T_{u,d}^{\text{dec,G}_3,\text{sat}}(k_d) &= \frac{v_{u,d}^{\text{middle,sat,1}}(k_d) - v_{u,d}^{\text{free}}}{a_{u,d}^{\text{dec}}} + \frac{v_{u,d}^{\text{idling}} - v_{u,d}^{\text{middle,sat,2}}(k_d)}{a_{u,d}^{\text{dec}}}. \end{aligned} \tag{65}$$

- For the accelerating behavior, we have

$$\begin{aligned} n_{u,d}^{\text{acc,G}_1,\text{sat}}(k_d) &= n_{u,d}^{\text{G}_1,\text{sat}}(k_d), \\ n_{u,d}^{\text{acc,G}_2,\text{sat}}(k_d) &= n_{u,d}^{\text{G}_2,\text{sat}}(k_d), \\ n_{u,d}^{\text{acc,G}_3,\text{sat}}(k_d) &= n_{u,d}^{\text{G}_3,\text{sat}}(k_d), \end{aligned} \tag{66}$$

and

$$\begin{aligned} T_{u,d}^{\text{acc,G}_1,\text{sat}}(k_d) &= \frac{v_{u,d}^{\text{free}} - v_{u,d}^{\text{idling}}}{a_{u,d}^{\text{acc}}}, \\ T_{u,d}^{\text{acc,G}_2,\text{sat}}(k_d) &= \frac{v_{u,d}^{\text{free}} - v_{u,d}^{\text{idling}}}{a_{u,d}^{\text{acc}}}, \\ T_{u,d}^{\text{acc,G}_3,\text{sat}}(k_d) &= \frac{v_{u,d}^{\text{middle,sat,2}}(k_d) - v_{u,d}^{\text{middle,sat,1}}(k_d)}{a_{u,d}^{\text{acc}}}. \end{aligned} \tag{67}$$

Now, we explain in more details how the equations presented above are obtained. Since $\alpha_{u,d}^{\text{arrive,q}}(k_d) < \mu_{u,d}$, i.e., the arriving flow of the vehicles is less than the leaving flow rates, the temporal distance between the arrival times of two successive vehicles in group 2 should be less than the temporal distance between the leaving times. This implies that for each vehicle in group 2 compared with its predecessor, the length of the idling behavior will be reduced in the time-speed curve. Figure 4(a), illustrating the time-speed curves of the first, last, and representative vehicle of group 2, is obtained based on this fact. From this figure, the arrival time of the vehicles in group 2 (i.e., the time period between the arrival instant of the first and the last vehicle) for the saturated scenario is

$$T_{u,d}^{\text{arrive,G}_2,\text{sat}}(k_d) = c_d - T_{\text{last}}^{\text{total,G}_2,\text{sat}}(k_d). \tag{68}$$

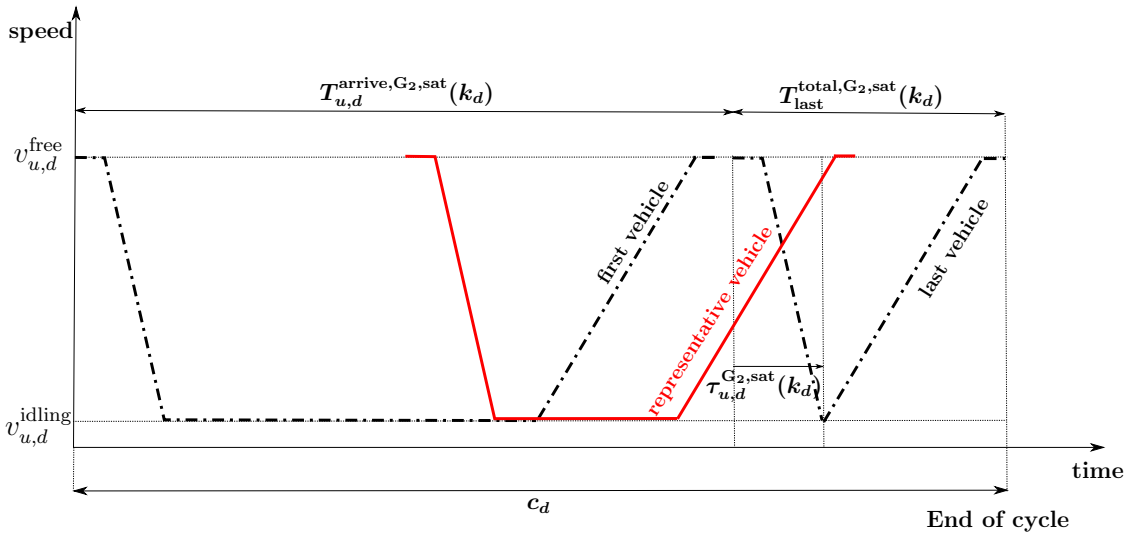

(a) Traffic behaviors for the first, last, and representative vehicle in group 2

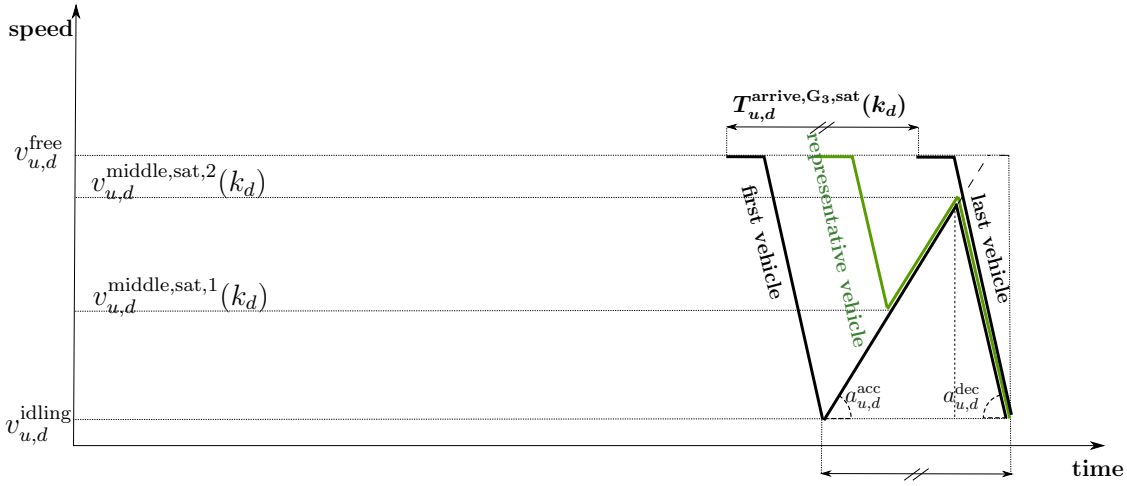

(b) Traffic behaviors for the first, last, and representative vehicle in group 3

Figure 4: Traffic behavior of different groups for **saturated** urban traffic scenario, **case 1**

Moreover, for the last vehicle in group 2, from Lemma 3.1 for the accelerating and for the free-flow behavior at the end, we can write

$$\frac{\left(n_{u,d}^{\text{G}_1,\text{sat}}(k_d)+n_{u,d}^{\text{G}_2,\text{sat}}(k_d)\right)l^{\text{veh}}}{N_{u,d}^{\text{lane}}} = v_{u,d}^{\text{free}}\cdot T^{\text{free,end}}+ \frac{a_{u,d}^{\text{acc}}}{2}\left(\frac{v_{u,d}^{\text{free}}-v_{u,d}^{\text{idling}}}{a_{u,d}^{\text{acc}}}\right)^2+v_{u,d}^{\text{idling}}\left(\frac{v_{u,d}^{\text{free}}-v_{u,d}^{\text{idling}}}{a_{u,d}^{\text{acc}}}\right), \tag{69}$$

from which $T^{\text{free,end}}$ is found. Moreover,

$$T_{\text{last}}^{\text{total,G}_2,\text{sat}}(k_d)=\tau_{u,d}^{\text{G}_2,\text{sat}}(k_d)+\frac{v_{u,d}^{\text{free}}-v_{u,d}^{\text{idling}}}{a_{u,d}^{\text{acc}}}+T^{\text{free,end}}, \tag{70}$$

and

$$n_{u,d}^{\text{G}_2,\text{sat}}(k_d)=\alpha_{u,d}^{\text{arrive,q}}(k_d)T_{u,d}^{\text{arrive,G}_2,\text{sat}}(k_d). \tag{71}$$

By substituting (70) into (68) and (71) into the expression for $T^{\text{free,end}}$ resulted by (69), (58) is obtained.

Next, we explain how (53) and (54) are obtained. We consider the time-speed curves of the first, the last, and the representative vehicle in group 3 (see Figure 4(b)). Since $v_{u,d}^{\text{middle,sat,1}}(k_d)$ corresponds to the average behavior of group 3, we consider it as the average of $v_{u,d}^{\text{idling}}$ corresponding to the first vehicle and $v_{u,d}^{\text{middle,sat,2}}(k_d)$ corresponding to the last vehicle (see (53)). For $v_{u,d}^{\text{middle,sat,2}}(k_d)$, we start by

$$n_{u,d}^{\text{sat}}(k_d) = \sum_{i=1}^{3} n_{u,d}^{\text{G}_i,\text{sat}}(k_d), \tag{72}$$

where $n_{u,d}^{\text{sat}}(k_d)$ is computed by the flow model. We can write

$$T_{u,d}^{\text{arrive,G}_3,\text{sat}}(k_d) = \frac{n_{u,d}^{\text{G}_3,\text{sat}}(k_d)}{\alpha_{u,d}^{\text{arrive,q}}(k_d)}. \tag{73}$$

Moreover, from Figure 4(b) we have

$$\begin{aligned} T_{u,d}^{\text{arrive,G}_3,\text{sat}}(k_d) =& \frac{v_{u,d}^{\text{middle,sat,2}}(k_d) - v_{u,d}^{\text{idling}}}{a_{u,d}^{\text{acc}}} + \frac{v_{u,d}^{\text{idling}} - v_{u,d}^{\text{middle,sat,2}}(k_d)}{a_{u,d}^{\text{dec}}} \\ =& \left(v_{u,d}^{\text{middle,sat,2}}(k_d) - v_{u,d}^{\text{idling}}\right)\left(\frac{1}{a_{u,d}^{\text{acc}}} - \frac{1}{a_{u,d}^{\text{dec}}}\right). \end{aligned} \tag{74}$$

Therefore, we obtain (54), i.e.,

$$v_{u,d}^{\text{middle,sat,2}}(k_d) = v_{u,d}^{\text{idling}} + \frac{n_{u,d}^{\text{G}_3,\text{sat}}(k_d)}{\alpha_{u,d}^{\text{arrive,q}}(k_d)}\left(\frac{a_{u,d}^{\text{acc}} a_{u,d}^{\text{dec}}}{a_{u,d}^{\text{dec}} - a_{u,d}^{\text{acc}}}\right). \tag{75}$$

However, there is no guarantee yet that $v_{u,d}^{\text{middle,sat,2}}(k_d)$ given by (75) does never exceed $v_{u,d}^{\text{free}}$. Defining $n_{u,d}^{\text{G}_2,\text{sat}}(k_d)$ by (56) provides us with this guarantee, since $v_{u,d}^{\text{middle,sat,2}}(k_d) \leq v_{u,d}^{\text{free}}$ implies that

$$\left(v_{u,d}^{\text{middle,sat,2}}(k_d) - v_{u,d}^{\text{idling}}\right)\left(\frac{1}{a_{u,d}^{\text{acc}}} - \frac{1}{a_{u,d}^{\text{dec}}}\right) \leq \left(v_{u,d}^{\text{free}} - v_{u,d}^{\text{idling}}\right)\left(\frac{1}{a_{u,d}^{\text{acc}}} - \frac{1}{a_{u,d}^{\text{dec}}}\right), \tag{76}$$

with the left-hand side of (76) equal to $T_{u,d}^{\text{arrive,G}_3,\text{sat}}(k_d)$ (see (74)). Hence, from (73) we obtain

$$n_{u,d}^{\text{G}_3,\text{sat}}(k_d) \leq \alpha_{u,d}^{\text{arrive,q}}(k_d)\left(v_{u,d}^{\text{free}} - v_{u,d}^{\text{idling}}\right)\left(\frac{1}{a_{u,d}^{\text{acc}}} - \frac{1}{a_{u,d}^{\text{dec}}}\right). \tag{77}$$

Finally, from (72) and (77) we obtain (56). Moreover, (56) together with (72) results in (77); (77) yields (76), which itself implies that $v_{u,d}^{\text{middle,sat,2}}(k_d) \leq v_{u,d}^{\text{free}}$ should hold.

5.2 Case 2: $\alpha_{u,d}^{\text{arrive,q}}(k_d) \geq \mu_{u,d}$

For the second case of the saturated urban traffic scenario, i.e., for $\alpha_{u,d}^{\text{arrive,q}}(k_d) \geq \mu_{u,d}$, the vehicles observed during one cycle are divided into four groups:

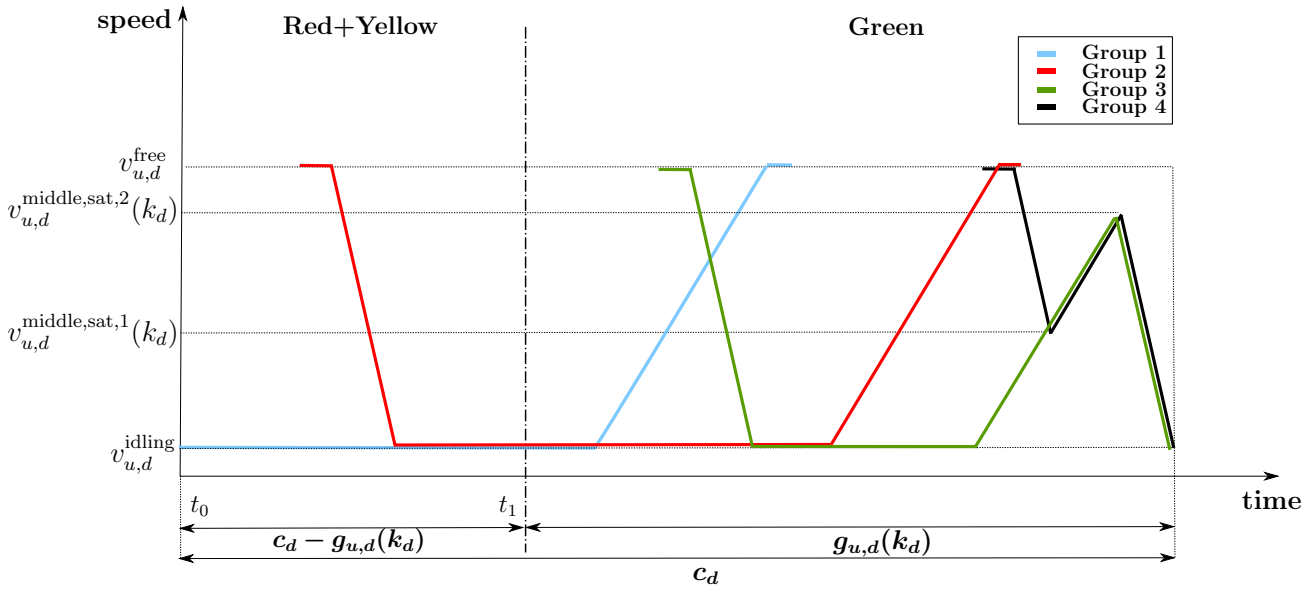

Figure 5: Traffic behaviors on link (u, d) within one cycle for the **saturated** urban traffic scenario, case 2: $\alpha_{u,d}^{\text{arrive,q}}(k_d) \geq \mu_{u,d}$

Group 1: composed of those vehicles that are already in the link standing in a queue at the beginning of the cycle (see the blue curve in Figure 5 for the average behavior of this group); the average behavior of this group is exactly similar to that of the first group for case 1 of the saturated scenario (see Section 5.1).

Group 2: composed of those vehicles that arrive at the tail of the waiting queue during the current cycle after they decelerate from $v_{u,d}^{\text{free}}$ to $v_{u,d}^{\text{idling}}$. They idle for a while behind the initial queue, and then accelerate just after the queue in front of them has been dissolved. They finally leave the link during the current cycle (see the red curve in Figure 5 for the average behavior of this group). The observed behavior for this group of vehicles is similar to the observed behavior for group 2 for case 1 of the saturated scenario (see Section 5.1), except that for the same queue number and green time values, the representative vehicle of group 2 shows an idling behavior for a longer period compared with case 1 (compare Figures 3 and 5).

Group 3: composed of those vehicles that should decelerate after a while as they approach the idling queue in front of them consisting of the vehicles in group 1 and group 2 (see the green curve in Figure 5 for the average behavior of this group). They reach $v_{u,d}^{\text{idling}}$, idle for a while, and then accelerate to reach $v_{u,d}^{\text{middle,sat,2}}(k_d)$ when they notice that there is not enough time to reach and pass the traffic light. Hence, they decelerate to $v_{u,d}^{\text{idling}}$. The value of $v_{u,d}^{\text{middle,sat,2}}$ is given by

$$v_{u,d}^{\text{middle,sat,2}}(k_d) = v_{u,d}^{\text{idling}} + \frac{a_{u,d}^{\text{acc}} a_{u,d}^{\text{dec}}}{a_{u,d}^{\text{dec}} - a_{u,d}^{\text{acc}}} \cdot \left(c_d - \frac{n_{u,d}^{\text{G2,sat}}(k_d) + n_{u,d}^{\text{G3,sat}}(k_d)}{\alpha_{u,d}^{\text{arrive,q}}(k_d)} - \frac{C_{u,d} - n_{u,d}^{\text{G1,sat}}(k_d) - n_{u,d}^{\text{G2,sat}}(k_d) - n_{u,d}^{\text{G3,sat}}(k_d)}{N_{u,d}^{\text{lane}} v_{u,d}^{\text{free}}} l^{\text{veh}} + \frac{\left(v_{u,d}^{\text{free}} - v_{u,d}^{\text{idling}}\right)^2}{2 a_{u,d}^{\text{acc}} v_{u,d}^{\text{free}}} \right). \tag{78}$$

Group 4: composed of those vehicles that arrive at the tail of the queue consisting of the vehicles in groups 1, 2, and 3, when the queue has already started to move forward

(see the black curve in Figure 5 for the average behavior of vehicles in group 4). Hence, as they approach the moving queue they decelerate to reach $v_{u,d}^{\text{middle,sat,1}}(k_d)$ given by

$$v_{u,d}^{\text{middle,sat,1}}(k_d) = \frac{v_{u,d}^{\text{idling}} + v_{u,d}^{\text{middle,sat,2}}(k_d)}{2}. \tag{79}$$

Then they accelerate with the queue until they reach $v_{u,d}^{\text{middle,sat,2}}(k_d)$. At this moment, since the vehicles in group 3 in front of them start to decelerate, the vehicles in group 4 will follow the same behavior and decelerate to $v_{u,d}^{\text{idling}}$.

For the number of vehicles in each of the groups, we have

$$n_{u,d}^{\text{G}_1,\text{sat}}(k_d) = q_{u,d}(k_d), \tag{80}$$

$$n_{u,d}^{\text{G}_2,\text{sat}}(k_d) = \min\left\{\alpha_{u,d}^{\text{arrive,q}}(k_d)\cdot T_{u,d}^{\text{arrive,G}_2,\text{sat}}(k_d), n_{u,d}^{\text{sat}}(k_d) - n_{u,d}^{\text{G}_1,\text{sat}}(k_d)\right\}, \tag{81}$$

$$\begin{aligned} n_{u,d}^{\text{G}_3,\text{sat}}(k_d) = \min\Bigg\{ & \alpha_{u,d}^{\text{arrive,q}}(k_d)\cdot T_{u,d}^{\text{arrive,G}_3,\text{sat}}(k_d), \\ & \frac{\left(v_{u,d}^{\text{free}}\right)^2 - \left(v_{u,d}^{\text{idling}}\right)^2}{l^{\text{veh}}} N_{u,d}^{\text{lane}}\left(\frac{1}{a_{u,d}^{\text{acc}}} - \frac{1}{a_{u,d}^{\text{dec}}}\right) - n_{u,d}^{\text{G}_1,\text{sat}}(k_d) - n_{u,d}^{\text{G}_2,\text{sat}}(k_d)\Bigg\}, \end{aligned} \tag{82}$$

$$n_{u,d}^{\text{G}_4,\text{sat}}(k_d) = n_{u,d}^{\text{sat}}(k_d) - \sum_{i=1}^{3} n_{u,d}^{\text{G}_i,\text{sat}}(k_d), \tag{83}$$

with $T_{u,d}^{\text{arrive,G}_2,\text{sat}}(k_d)$ and $T_{u,d}^{\text{arrive,G}_3,\text{sat}}(k_d)$ computed by

$$\begin{aligned} T_{u,d}^{\text{arrive,G}_2,\text{sat}}(k_d) = & \frac{N_{u,d}^{\text{lane}} v_{u,d}^{\text{free}}}{\frac{2\alpha_{u,d}^{\text{arrive,q}}(k_d)}{\mu_{u,d}} N_{u,d}^{\text{lane}} v_{u,d}^{\text{free}} + \alpha_{u,d}^{\text{arrive,q}}(k_d) l^{\text{veh}}} \cdot \\ & \left(g_{u,d}(k_d) - \frac{n_{u,d}^{\text{G}_1,\text{sat}}(k_d) l^{\text{veh}}}{N_{u,d}^{\text{lane}} v_{u,d}^{\text{free}}} - \frac{\left(v_{u,d}^{\text{free}} - v_{u,d}^{\text{idling}}\right)^2}{2 v_{u,d}^{\text{free}} a_{u,d}^{\text{acc}}}\right), \end{aligned} \tag{84}$$

$$\begin{aligned} T_{u,d}^{\text{arrive,G}_3,\text{sat}}(k_d) = & \frac{\left(v_{u,d}^{\text{middle,sat,2}}(k_d)\right)^2 - \left(v_{u,d}^{\text{idling}}\right)^2}{\alpha_{u,d}^{\text{arrive,q}}(k_d) l^{\text{veh}}} N_{u,d}^{\text{lane}}\left(\frac{1}{a_{u,d}^{\text{acc}}} - \frac{1}{a_{u,d}^{\text{dec}}}\right) \\ & - T_{u,d}^{\text{arrive,G}_2,\text{sat}}(k_d) - \frac{n_{u,d}^{\text{G}_1,\text{sat}}(k_d)}{\alpha_{u,d}^{\text{arrive,q}}(k_d)}, \end{aligned} \tag{85}$$

and $\tau_{u,d}^{\text{G}_2,\text{sat}}(k_d)$ by (21). Note that we should use the minimum function in (81) and (82) to make sure that the number of vehicles is positive and also that $v_{u,d}^{\text{middle,sat,2}}(k_d)$ does not exceed $v_{u,d}^{\text{free}}$ (for more details we refer the readers to the explanations given in Section 5.1 for case 1).

The number of vehicles in each group that show a specific behavior and the time duration of each behavior for case 2 of the urban saturated scenario is given next:

- For the free-flow behavior, we have

$$\begin{aligned} n_{u,d}^{\text{free,G}_1,\text{sat}}(k_d) &= n_{u,d}^{\text{G}_1,\text{sat}}(k_d), \\ n_{u,d}^{\text{free,G}_2,\text{sat}}(k_d) &= n_{u,d}^{\text{G}_2,\text{sat}}(k_d), \\ n_{u,d}^{\text{free,G}_3,\text{sat}}(k_d) &= n_{u,d}^{\text{G}_3,\text{sat}}(k_d), \\ n_{u,d}^{\text{free,G}_4,\text{sat}}(k_d) &= n_{u,d}^{\text{G}_4,\text{sat}}(k_d), \end{aligned} \tag{86}$$

and

$$\begin{aligned} T_{u,d}^{\text{free,G}_1,\text{sat}}(k_d) &= \frac{\left(n_{u,d}^{\text{G}_1,\text{sat}}(k_d) + 0.5 n_{u,d}^{\text{G}_2,\text{sat}}(k_d)\right) l^{\text{veh}}}{v_{u,d}^{\text{free}}} - \frac{\left(v_{u,d}^{\text{free}}\right)^2 - \left(v_{u,d}^{\text{idling}}\right)^2}{2 a_{u,d}^{\text{acc}} v_{u,d}^{\text{free}}}, \\ T_{u,d}^{\text{free,G}_2,\text{sat}}(k_d) &= \tau_{u,d}^{\text{G}_2,\text{sat}}(k_d) - \frac{v_{u,d}^{\text{idling}} - v_{u,d}^{\text{free}}}{a_{u,d}^{\text{dec}}} + T_{u,d}^{\text{free,G}_1,\text{sat}}(k_d), \\ T_{u,d}^{\text{free,G}_3,\text{sat}}(k_d) &= \tau_{u,d}^{\text{G}_3,\text{sat}}(k_d) - \frac{v_{u,d}^{\text{idling}} - v_{u,d}^{\text{free}}}{a_{u,d}^{\text{dec}}}, \\ T_{u,d}^{\text{free,G}_4,\text{sat}}(k_d) &= \tau_{u,d}^{\text{G}_4,\text{sat}}(k_d) - \frac{v_{u,d}^{\text{middle,sat,1}}(k_d) - v_{u,d}^{\text{free}}}{a_{u,d}^{\text{dec}}}, \end{aligned} \tag{87}$$

with $\tau_{u,d}^{\text{G}_3,\text{sat}}(k_d)$ computed by(61).

- For the idling behavior, we have

$$\begin{aligned} n_{u,d}^{\text{idling,G}_1,\text{sat}}(k_d) &= n_{u,d}^{\text{G}_1,\text{sat}}(k_d), \\ n_{u,d}^{\text{idling,G}_2,\text{sat}}(k_d) &= n_{u,d}^{\text{G}_2,\text{sat}}(k_d), \\ n_{u,d}^{\text{idling,G}_3,\text{sat}}(k_d) &= n_{u,d}^{\text{G}_3,\text{sat}}(k_d), \\ n_{u,d}^{\text{idling,G}_4,\text{sat}}(k_d) &= 0, \end{aligned} \tag{88}$$

and

$$\begin{aligned} T_{u,d}^{\text{idling,G}_1,\text{sat}}(k_d) &= c_d - g_{u,d}(k_d) + \frac{0.5 n_{u,d}^{\text{G}_1,\text{sat}}(k_d)}{\mu_{u,d}}, \\ T_{u,d}^{\text{idling,G}_2,\text{sat}}(k_d) &= c_d - g_{u,d}(k_d) + \frac{n_{u,d}^{\text{G}_1,\text{sat}}(k_d)}{\mu_{u,d}} - \tau_{u,d}^{\text{G}_2,\text{sat}}(k_d) + \\ &\qquad 0.5 n_{u,d}^{\text{idling,G}_2,\text{sat}}(k_d) \left(\frac{1}{\mu_{u,d}} - \frac{1}{\alpha_{u,d}^{\text{arrive,q}}(k_d)}\right), \\ T_{u,d}^{\text{idling,G}_3,\text{sat}}(k_d) &= 0.5 \left(c_d - g_{u,d}(k_d) + \frac{n_{u,d}^{\text{G}_1,\text{sat}}(k_d)}{\mu_{u,d}} - \tau_{u,d}^{\text{G}_2,\text{sat}}(k_d) + \right. \\ &\qquad \left. n_{u,d}^{\text{idling,G}_2,\text{sat}}(k_d) \left(\frac{1}{\mu_{u,d}} - \frac{1}{\alpha_{u,d}^{\text{arrive,q}}(k_d)}\right)\right), \\ T_{u,d}^{\text{idling,G}_4,\text{sat}}(k_d) &= 0. \end{aligned} \tag{89}$$

- For the decelerating behavior, we have

$$\begin{aligned} n_{u,d}^{\text{dec,G}_1,\text{sat}}(k_d) &= 0, \\ n_{u,d}^{\text{dec,G}_2,\text{sat}}(k_d) &= n_{u,d}^{\text{G}_2,\text{sat}}(k_d), \\ n_{u,d}^{\text{dec,G}_3,\text{sat}}(k_d) &= n_{u,d}^{\text{G}_3,\text{sat}}(k_d), \\ n_{u,d}^{\text{dec,G}_4,\text{sat}}(k_d) &= n_{u,d}^{\text{G}_4,\text{sat}}(k_d), \end{aligned} \tag{90}$$

and

$$
\begin{aligned}
T_{u,d}^{\mathrm{dec,G_1,sat}}(k_d) &= 0,\\
T_{u,d}^{\mathrm{dec,G_2,sat}}(k_d) &= \frac{v_{u,d}^{\mathrm{idling}} - v_{u,d}^{\mathrm{free}}}{a_{u,d}^{\mathrm{dec}}},\\
T_{u,d}^{\mathrm{acc,G_3,sat}}(k_d) &= \frac{v_{u,d}^{\mathrm{idling}}(k_d) - v_{u,d}^{\mathrm{free}}(k_d)}{a_{u,d}^{\mathrm{dec}}} + \frac{v_{u,d}^{\mathrm{idling}}(k_d) - v_{u,d}^{\mathrm{middle,sat,2}}(k_d)}{a_{u,d}^{\mathrm{dec}}},\\
T_{u,d}^{\mathrm{dec,G_4,sat}}(k_d) &= \frac{v_{u,d}^{\mathrm{middle,sat,1}}(k_d) - v_{u,d}^{\mathrm{free}}}{a_{u,d}^{\mathrm{dec}}} + \frac{v_{u,d}^{\mathrm{idling}} - v_{u,d}^{\mathrm{middle,sat,2}}(k_d)}{a_{u,d}^{\mathrm{dec}}}.
\end{aligned}
\tag{91}
$$

- For the accelerating behavior, we have

$$
\begin{aligned}
n_{u,d}^{\mathrm{acc,G_1,sat}}(k_d) &= n_{u,d}^{\mathrm{G_1,sat}}(k_d),\\
n_{u,d}^{\mathrm{acc,G_2,sat}}(k_d) &= n_{u,d}^{\mathrm{G_2,sat}}(k_d),\\
n_{u,d}^{\mathrm{acc,G_3,sat}}(k_d) &= n_{u,d}^{\mathrm{G_3,sat}}(k_d),\\
n_{u,d}^{\mathrm{acc,G_4,sat}}(k_d) &= n_{u,d}^{\mathrm{G_4,sat}}(k_d),
\end{aligned}
\tag{92}
$$

and

$$
\begin{aligned}
T_{u,d}^{\mathrm{acc,G_1,sat}}(k_d) &= \frac{v_{u,d}^{\mathrm{free}} - v_{u,d}^{\mathrm{idling}}}{a_{u,d}^{\mathrm{acc}}},\\
T_{u,d}^{\mathrm{acc,G_2,sat}}(k_d) &= \frac{v_{u,d}^{\mathrm{free}} - v_{u,d}^{\mathrm{idling}}}{a_{u,d}^{\mathrm{acc}}},\\
T_{u,d}^{\mathrm{acc,G_3,sat}}(k_d) &= \frac{v_{u,d}^{\mathrm{idling}}(k_d) - v_{u,d}^{\mathrm{middle,sat,2}}(k_d)}{a_{u,d}^{\mathrm{acc}}},\\
T_{u,d}^{\mathrm{acc,G_4,sat}}(k_d) &= \frac{v_{u,d}^{\mathrm{middle,sat,2}}(k_d) - v_{u,d}^{\mathrm{middle,sat,1}}(k_d)}{a_{u,d}^{\mathrm{acc}}}.
\end{aligned}
\tag{93}
$$

Next we explain in more details how the equations given in this section are derived considering the time-speed curves of each group of vehicles for case 2 of the saturated scenario. Figure 6 illustrates the time-speed curves of the first, last, and representative vehicle in groups 2, 3, and 4 for case 2 of the saturated urban traffic scenario (the time-speed curves of the vehicles in group 1 are not shown, since they are the same as for case 1). Since for case 2 we have $\alpha_{u,d}^{\mathrm{arrive,q}}(k_d) \geq \mu_{u,d}$, the temporal distance between the starting point of the time-speed curves of every two successive vehicles in group 2 should be greater than or equal to the temporal distance between the endpoints of the curves. This implies that the idling time of a vehicle in group 2 compared with its predecessor increases.

For the first vehicle in group 2 (see Figure 6(a)), the time-speed curve includes the below-mentioned behaviors for the given time durations:

- free-flow (start) + decelerating:

$$
\tau_{u,d}^{\mathrm{G_2,sat}}(k_d),
\tag{94}
$$

  where $\tau_{u,d}^{\mathrm{G_2,sat}}(k_d)$ is computed by (21).

- idling (the idling time of the first vehicle in group 2 is in the limit equal to the idling time of the last vehicle in group 1 minus $\tau_{u,d}^{\mathrm{G_2,sat}}(k_d)$):

$$
c_d - g_{u,d}(k_d) + \frac{n_{u,d}^{\mathrm{G_1,sat}}(k_d)}{\mu_{u,d}} - \tau_{u,d}^{\mathrm{G_2,sat}}(k_d);
\tag{95}
$$

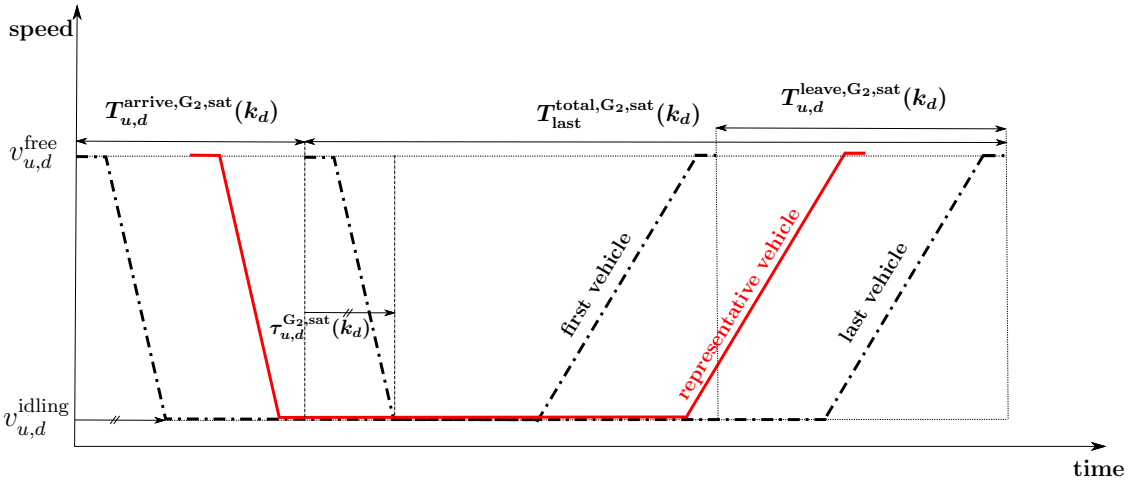

(a) Traffic behaviors for the first, last, and representative vehicle in group 2

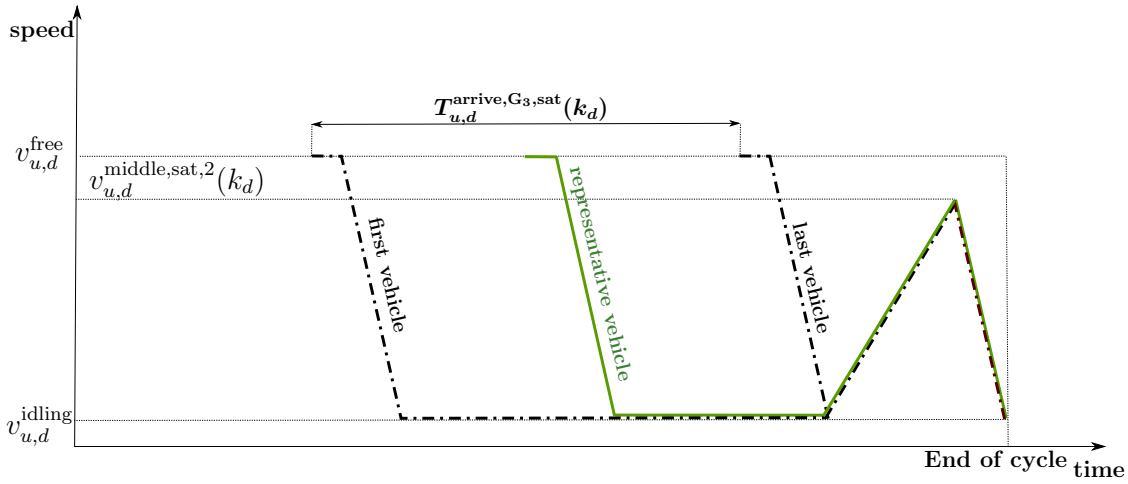

(b) Traffic behaviors for the first, last, and representative vehicle in group 3

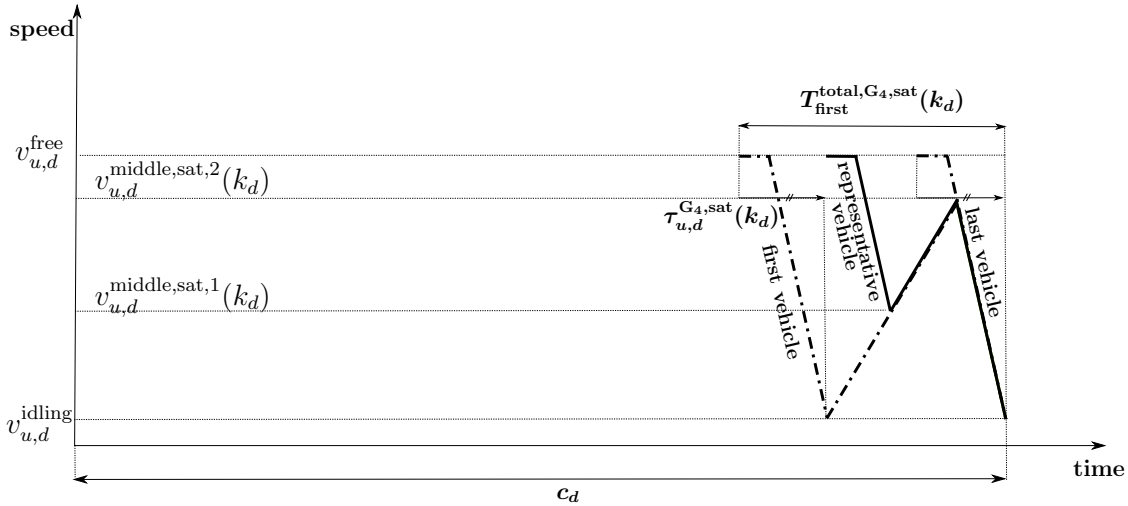

(c) Traffic behaviors for the first, last, and representative vehicle in group 4

Figure 6: Traffic behavior of different groups for **saturated** urban traffic scenario, **Case 2**

- accelerating:

$$\frac{v_{u,d}^{\text{free}} - v_{u,d}^{\text{idling}}}{a_{u,d}^{\text{acc}}}; \tag{96}$$

- free-flow (end)[8]:

$$\frac{n_{u,d}^{\text{G}_1,\text{sat}}(k_d)}{N_{u,d}^{\text{lane}} v_{u,d}^{\text{free}}} l^{\text{veh}} - \frac{\left(v_{u,d}^{\text{free}}\right)^2 - \left(v_{u,d}^{\text{idling}}\right)^2}{2 a_{u,d}^{\text{acc}} v_{u,d}^{\text{free}}}. \tag{97}$$

Similarly, for the last vehicle in group 2, we can see that the time duration of each behavior is the same as for the first vehicle, except for the idling and for the free-flow behavior at the end, where we have

- idling:

$$c_d - g_{u,d}(k_d) + \frac{n_{u,d}^{\text{G}_1,\text{sat}}(k_d)}{\mu_{u,d}} - \tau_{u,d}^{\text{G}_2,\text{sat}}(k_d) + n_{u,d}^{\text{G}_2,\text{sat}}(k_d) \left(\frac{1}{\mu_{u,d}} - \frac{1}{\alpha_{u,d}^{\text{arrive,q}}(k_d)} \right). \tag{98}$$

  Note that the last term in (98) shows that for case 2, the idling time of the vehicles in group 2 increases gradually for each two successive vehicles. To obtain this term, from the fact that the leaving flow rate of the vehicles in a saturated urban traffic scenario is $\mu_{u,d}$, we can write

$$\alpha_{u,d}^{\text{arrive,q}}(k_d) = \frac{n_{u,d}^{\text{G}_2,\text{sat}}(k_d)}{T_{u,d}^{\text{arrive,G}_2,\text{sat}}(k_d)}, \tag{99}$$

  and

$$\mu_{u,d} = \frac{n_{u,d}^{\text{G}_2,\text{sat}}(k_d)}{T_{u,d}^{\text{leave,G}_2,\text{sat}}(k_d)}. \tag{100}$$

  with $T_{u,d}^{\text{leave,G}_2,\text{sat}}(k_d)$ the time duration that vehicles in group 2 need to leave the link (see Figure 6(a)). Moreover, the difference between $T_{u,d}^{\text{arrive,G}_2,\text{sat}}(k_d)$ and $T_{u,d}^{\text{leave,G}_2,\text{sat}}(k_d)$ shows the excess time that the last vehicle in group 2 spends idling within the queue w.r.t. the first vehicle. Therefore, the last term in (98) is obtained.

- free-flow (end):

$$\frac{\left(n_{u,d}^{\text{G}_1,\text{sat}}(k_d) + n_{u,d}^{\text{G}_2,\text{sat}}(k_d)\right)}{N_{u,d}^{\text{lane}} v_{u,d}^{\text{free}}} l^{\text{veh}} - \frac{\left(v_{u,d}^{\text{free}}\right)^2 - \left(v_{u,d}^{\text{idling}}\right)^2}{2 a_{u,d}^{\text{acc}} v_{u,d}^{\text{free}}}. \tag{101}$$

Now we can also find an expression for $T_{u,d}^{\text{arrive,G}_2,\text{sat}}(k_d)$, $T_{u,d}^{\text{arrive,G}_3,\text{sat}}(k_d)$, and $v_{u,d}^{\text{middle,sat,2}}(k_d)$. From Figures 6(a) for $T_{u,d}^{\text{arrive,G}_2,\text{sat}}(k_d)$ we can write

$$T_{u,d}^{\text{arrive,G}_2,\text{sat}}(k_d) = c_d - T_{\text{last}}^{\text{total,G}_2,\text{sat}}(k_d). \tag{102}$$

[8]The number of vehicles in front of the first vehicle in group 1 is considered to be equal to $n_{u,d}^{\text{G}_1,\text{sat}}(k_d)$.

Hence,

$$T_{u,d}^{\text{arrive,G}_2,\text{sat}}(k_d) = c_d - \tau_{u,d}^{\text{G}_2,\text{sat}}(k_d) - c_d + g_{u,d}(k_d) - \frac{n_{u,d}^{\text{G}_2,\text{sat}}(k_d)}{\mu_{u,d}} + \tau_{u,d}^{\text{G}_2,\text{sat}}(k_d) - n_{u,d}^{\text{G}_2,\text{sat}}(k_d)\left(\frac{1}{\mu_{u,d}} - \frac{1}{\alpha_{u,d}^{\text{arrive,q}}(k_d)}\right) - \frac{v_{u,d}^{\text{free}} - v_{u,d}^{\text{idling}}}{a_{u,d}^{\text{acc}}} - \frac{\left(n_{u,d}^{\text{G}_1,\text{sat}}(k_d) + n_{u,d}^{\text{G}_2,\text{sat}}(k_d)\right)}{N_{u,d}^{\text{lane}} v_{u,d}^{\text{free}}} l^{\text{veh}} + \frac{\left(v_{u,d}^{\text{free}}\right)^2 - \left(v_{u,d}^{\text{idling}}\right)^2}{2a_{u,d}^{\text{acc}} v_{u,d}^{\text{free}}}, \tag{103}$$

with

$$n_{u,d}^{\text{G}_2,\text{sat}}(k_d) = \alpha_{u,d}^{\text{arrive,q}}(k_d) \cdot T_{u,d}^{\text{arrive,G}_2,\text{sat}}(k_d). \tag{104}$$

From (102), (103), and (104), (84) is found.

From Figures 6(a), 6(b), and 6(c), we have

$$T_{u,d}^{\text{arrive,G}_2,\text{sat}}(k_d) + T_{u,d}^{\text{arrive,G}_3,\text{sat}}(k_d) + T_{u,d}^{\text{first,G}_4,\text{sat}}(k_d) = c_d. \tag{105}$$

Moreover, the first vehicle of group 4 should travel a distance of $\frac{C_{u,d} \cdot l^{\text{veh}}}{N_{u,d}^{\text{lane}}}$ in total during the current cycle. Hence, from Lemma 3.1 we can write

$$\left(n_{u,d}^{\text{G}_1,\text{sat}}(k_d) + n_{u,d}^{\text{G}_2,\text{sat}}(k_d) + n_{u,d}^{\text{G}_3,\text{sat}}(k_d)\right)\frac{l^{\text{veh}}}{N_{u,d}^{\text{lane}}} = \frac{1}{2}a_{u,d}^{\text{acc}}\left(\frac{v_{u,d}^{\text{middle,sat,2}}(k_d) - v_{u,d}^{\text{idling}}}{a_{u,d}^{\text{acc}}}\right)^2 + v_{u,d}^{\text{idling}}\left(\frac{v_{u,d}^{\text{middle,sat,2}}(k_d) - v_{u,d}^{\text{idling}}}{a_{u,d}^{\text{acc}}}\right) + \frac{1}{2}a_{u,d}^{\text{dec}}\left(\frac{v_{u,d}^{\text{idling}} - v_{u,d}^{\text{middle,sat,2}}(k_d)}{a_{u,d}^{\text{dec}}}\right)^2 + v_{u,d}^{\text{middle,sat,2}}(k_d)\left(\frac{v_{u,d}^{\text{idling}} - v_{u,d}^{\text{middle,sat,2}}(k_d)}{a_{u,d}^{\text{dec}}}\right). \tag{106}$$

Substituting $n_{u,d}^{\text{G}_2,\text{sat}}(k_d)$ by (104) and $n_{u,d}^{\text{G}_3,\text{sat}}(k_d)$ by

$$n_{u,d}^{\text{G}_3,\text{sat}}(k_d) = \alpha_{u,d}^{\text{arrive,q}}(k_d) \cdot T_{u,d}^{\text{arrive,G}_3,\text{sat}}(k_d), \tag{107}$$

we obtain (85).

Since for the first vehicle in group 4, we have

$$T_{u,d}^{\text{first,G}_4,\text{sat}}(k_d) = \tau_{u,d}^{\text{G}_4,\text{sat}}(k_d) + \left(v_{u,d}^{\text{middle,sat,2}}(k_d) - v_{u,d}^{\text{idling}}\right)\left(\frac{1}{a_{u,d}^{\text{acc}}} - \frac{1}{a_{u,d}^{\text{dec}}}\right), \tag{108}$$

with $\tau_{u,d}^{\text{G}_4,\text{sat}}(k_d)$ found similar to $\tau_{u,d}^{\text{G}_2,\text{sat}}(k_d)$ by

$$\tau_{u,d}^{\text{G}_4,\text{sat}}(k_d) = \frac{\left(C_{u,d} - n_{u,d}^{\text{G}_1,\text{sat}}(k_d) - n_{u,d}^{\text{G}_2,\text{sat}}(k_d) - n_{u,d}^{\text{G}_3,\text{sat}}(k_d)\right) l^{\text{veh}}}{N_{u,d}^{\text{lane}} v_{u,d}^{\text{free}}} - \frac{\left(v_{u,d}^{\text{idling}} - v_{u,d}^{\text{free}}\right)^2}{2a_{u,d}^{\text{dec}} v_{u,d}^{\text{free}}}, \tag{109}$$

from (105)-(109), (78) is obtained.

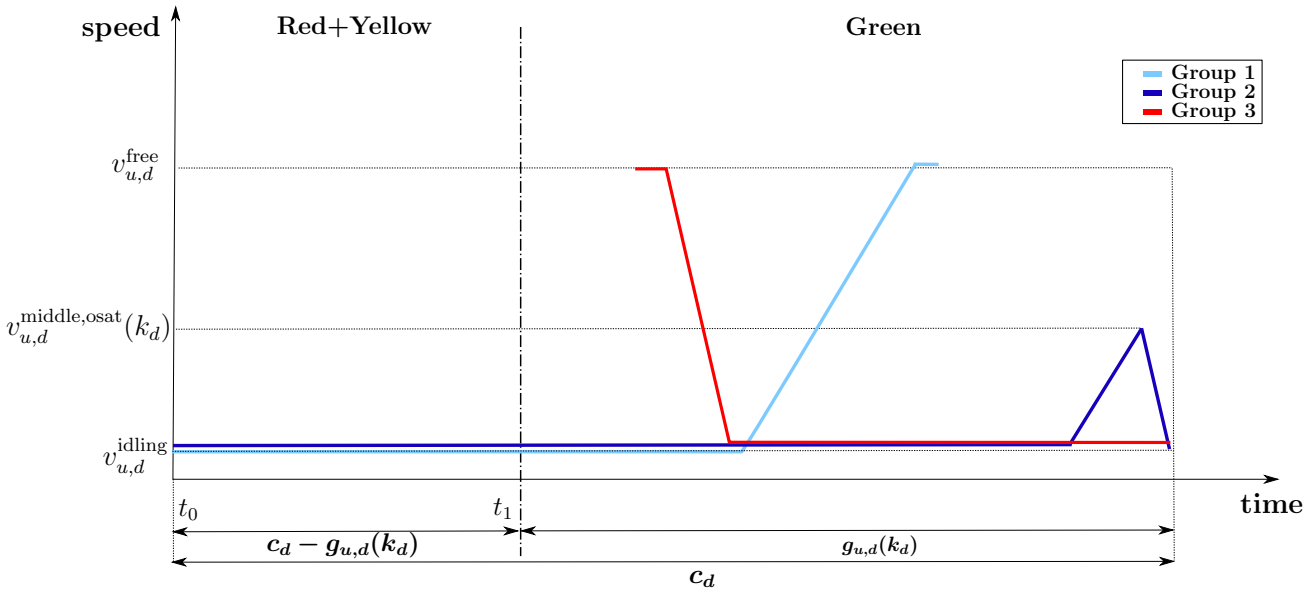

Figure 7: Traffic behaviors on link (u, d) within one cycle for the **over-saturated** urban traffic scenario

6 Flow-emission model for over-saturated scenario

For the over-saturated urban traffic scenario, not all the vehicles that are initially in the queue can leave the link within one cycle. Mathematically,

$$\sum_{o \in \mathcal{O}_{u,d}} \beta_{u,d,o} \cdot \mu_{u,d} \cdot g_{u,d,o}(k_d) < q_{u,d}(k_d). \tag{110}$$

Therefore, for this scenario we divide the vehicles that are observed in a link in the following three groups:

Group 1: composed of those vehicles in the queue that can leave the link during the current cycle (see the blue curve in Figure 7 for the average behavior of this group).

Group 2: composed of those vehicles in the queue that do not have enough time during the current cycle to pass through the traffic light (see the dark blue curve in Figure 7 for the average behavior of this group). These vehicles first accelerate as soon as the last vehicle in the queue in front of them composed of group 1 starts to move forward. However, since there is not enough time left for them to leave the link, after they reach $v_{u,d}^{\text{middle,osat}}(k_d)$ they decelerate to $v_{u,d}^{\text{idling}}$ and stop in front of the red light for at least another cycle time. We set

$$v_{u,d}^{\text{middle,osat}}(k_d) = v_{u,d}^{\text{idling}} + T_{u,d}^{\text{leave,osat,G}_1}(k_d) \frac{a_{u,d}^{\text{dec}} - a_{u,d}^{\text{acc}}}{2 a_{u,d}^{\text{dec}} a_{u,d}^{\text{acc}}}, \tag{111}$$

with

$$T_{u,d}^{\text{leave,osat,G}_1}(k_d) = \frac{\mu_{u,d} l^{\text{veh}} g_{u,d}(k_d)}{2 v_{u,d}^{\text{free}} + \mu_{u,d} l^{\text{veh}}} + \frac{\left(v_{u,d}^{\text{free}} - v_{u,d}^{\text{idling}}\right)^2}{a_{u,d}^{\text{acc}} \left(2 v_{u,d}^{\text{free}} + \mu_{u,d} l^{\text{veh}}\right)}. \tag{112}$$

Group 3: composed of the vehicles that arrive at the tail of the queue during the current cycle. These vehicles first decelerate and then idle for the rest of the cycle (see the red curve in Figure 7 for the average behavior of this group).

The leaving flow rate of the vehicles for the over-saturated scenario is the saturated leaving flow rate, $\mu_{u,d}$. Hence, for the number of vehicles in each of these three groups, we can write

$$n_{u,d}^{\mathrm{G}_1,\mathrm{osat}}(k_d) = \mu_{u,d}\left(g_{u,d}(k_d) - T_{u,d}^{\mathrm{leave,osat},\mathrm{G}_1}(k_d)\right), \tag{113}$$

$$n_{u,d}^{\mathrm{G}_2,\mathrm{osat}}(k_d) = q_{u,d}(k_d) - n_{u,d}^{\mathrm{G}_1,\mathrm{osat}}(k_d), \tag{114}$$

$$n_{u,d}^{\mathrm{G}_3,\mathrm{osat}}(k_d) = n_{u,d}^{\mathrm{osat}}(k_d) - \sum_{i=1}^{2} n_{u,d}^{\mathrm{G}_i,\mathrm{osat}}(k_d). \tag{115}$$

Next, we find the number of vehicles in each group that show a specific behavior, and also the time duration that each vehicle shows the behavior.

- For the free-flow behavior, we have

$$\begin{aligned} n_{u,d}^{\mathrm{free},\mathrm{G}_1,\mathrm{osat}}(k_d) &= n_{u,d}^{\mathrm{G}_1,\mathrm{osat}}(k_d), \\ n_{u,d}^{\mathrm{free},\mathrm{G}_2,\mathrm{osat}}(k_d) &= 0, \\ n_{u,d}^{\mathrm{free},\mathrm{G}_3,\mathrm{osat}}(k_d) &= n_{u,d}^{\mathrm{G}_3,\mathrm{osat}}(k_d), \end{aligned} \tag{116}$$

  and similarly to the under-saturated scenario,

$$\begin{aligned} T_{u,d}^{\mathrm{free},\mathrm{G}_1,\mathrm{osat}}(k_d) &= \frac{\mu_{u,d} l^{\mathrm{veh}} g_{u,d}(k_d)}{2v_{u,d}^{\mathrm{free}} + \mu_{u,d} l^{\mathrm{veh}}} - \frac{\left(v_{u,d}^{\mathrm{free}} - v_{u,d}^{\mathrm{idling}}\right)\left(\mu_{u,d} l^{\mathrm{veh}} + v_{u,d}^{\mathrm{free}} + v_{u,d}^{\mathrm{idling}}\right)}{a_{u,d}^{\mathrm{acc}}\left(2v_{u,d}^{\mathrm{free}} + \mu_{u,d} l^{\mathrm{veh}}\right)}, \\ T_{u,d}^{\mathrm{free},\mathrm{G}_2,\mathrm{osat}}(k_d) &= 0, \\ T_{u,d}^{\mathrm{free},\mathrm{G}_3,\mathrm{osat}}(k_d) &= \tau_{u,d}^{\mathrm{G}_3,\mathrm{osat}}(k_d) - \frac{v_{u,d}^{\mathrm{idling}} - v_{u,d}^{\mathrm{free}}}{a_{u,d}^{\mathrm{dec}}}, \end{aligned} \tag{117}$$

  with

$$\tau_{u,d}^{\mathrm{G}_3,\mathrm{osat}}(k_d) = \frac{\left(C_{u,d} - n_{u,d}^{\mathrm{G}_1,\mathrm{osat}}(k_d) - n_{u,d}^{\mathrm{G}_2,\mathrm{osat}}(k_d)\right) l^{\mathrm{veh}}}{N_{u,d}^{\mathrm{lane}} v_{u,d}^{\mathrm{free}}}. \tag{118}$$

- For the idling behavior, we have

$$\begin{aligned} n_{u,d}^{\mathrm{idling},\mathrm{G}_1,\mathrm{osat}}(k_d) &= n_{u,d}^{\mathrm{G}_1,\mathrm{osat}}(k_d), \\ n_{u,d}^{\mathrm{idling},\mathrm{G}_2,\mathrm{osat}}(k_d) &= n_{u,d}^{\mathrm{G}_2,\mathrm{osat}}(k_d), \\ n_{u,d}^{\mathrm{idling},\mathrm{G}_3,\mathrm{osat}}(k_d) &= n_{u,d}^{\mathrm{G}_3,\mathrm{osat}}(k_d), \end{aligned} \tag{119}$$

  and

$$\begin{aligned} T_{u,d}^{\mathrm{idling},\mathrm{G}_1,\mathrm{osat}}(k_d) &= c_d - g_{u,d}(k_d) + \frac{n_{u,d}^{\mathrm{G}_1,\mathrm{osat}}(k_d)}{2\mu_{u,d}}, \\ T_{u,d}^{\mathrm{idling},\mathrm{G}_2,\mathrm{osat}}(k_d) &= c_d - \frac{v_{u,d}^{\mathrm{free}} - v_{u,d}^{\mathrm{idling}}}{a_{u,d}^{\mathrm{acc}}}, \\ T_{u,d}^{\mathrm{idling},\mathrm{G}_3,\mathrm{osat}}(k_d) &= \frac{c_d - \tau_{u,d}^{\mathrm{G}_3,\mathrm{osat}}(k_d)}{2}. \end{aligned} \tag{120}$$

- For the decelerating behavior, we have

$$\begin{aligned} n_{u,d}^{\mathrm{dec},\mathrm{G}_1,\mathrm{osat}}(k_d) &= 0, \\ n_{u,d}^{\mathrm{dec},\mathrm{G}_2,\mathrm{osat}}(k_d) &= n_{u,d}^{\mathrm{G}_2,\mathrm{osat}}(k_d), \\ n_{u,d}^{\mathrm{dec},\mathrm{G}_3,\mathrm{osat}}(k_d) &= n_{u,d}^{\mathrm{G}_3,\mathrm{osat}}(k_d), \end{aligned} \tag{121}$$

and

$$\begin{aligned} T_{u,d}^{\mathrm{dec,G_1,osat}}(k_d) &= 0, \\ T_{u,d}^{\mathrm{dec,G_2,osat}}(k_d) &= \frac{v_{u,d}^{\mathrm{idling}} - v_{u,d}^{\mathrm{middle,osat}}(k_d)}{a_{u,d}^{\mathrm{dec}}}, \\ T_{u,d}^{\mathrm{dec,G_3,osat}}(k_d) &= \frac{v_{u,d}^{\mathrm{idling}} - v_{u,d}^{\mathrm{free}}}{a_{u,d}^{\mathrm{dec}}}. \end{aligned} \tag{122}$$

- For the accelerating behavior, we have

$$\begin{aligned} n_{u,d}^{\mathrm{acc,G_1,osat}}(k_d) &= n_{u,d}^{\mathrm{G_2,osat}}(k_d), \\ n_{u,d}^{\mathrm{acc,G_2,osat}}(k_d) &= n_{u,d}^{\mathrm{G_3,osat}}(k_d), \\ n_{u,d}^{\mathrm{acc,G_3,osat}}(k_d) &= 0, \end{aligned} \tag{123}$$

and

$$\begin{aligned} T_{u,d}^{\mathrm{acc,G_1,osat}}(k_d) &= \frac{v_{u,d}^{\mathrm{free}} - v_{u,d}^{\mathrm{idling}}}{a_{u,d}^{\mathrm{acc}}}, \\ T_{u,d}^{\mathrm{acc,G_2,osat}}(k_d) &= \frac{v_{u,d}^{\mathrm{middle,osat}}(k_d) - v_{u,d}^{\mathrm{idling}}}{a_{u,d}^{\mathrm{acc}}}, \\ T_{u,d}^{\mathrm{acc,G_3,osat}}(k_d) &= 0. \end{aligned} \tag{124}$$

Now we explain in more detail how the main equations given in this section are obtained. Figure 8 illustrates the time-speed curves of the first, last, and representative vehicle of groups 2 and 3 for the over-saturated urban scenario. The dashed line on the left-hand side in Figure 8(a) shows the time-speed curve of the first vehicle in group 1, and the dashed line on the right-hand side in this figure shows the time-speed curve of the last vehicle in group 1 that can still accelerate and leave the link. However, the next vehicle in the queue (i.e., the first vehicle in group 2) is the first vehicle in the queue that should necessarily decelerate after its speed reaches $v_{u,d}^{\mathrm{middle,first}}(k_d)$, so that it can stop in front of the red light at the end of the cycle.

Next, we compute $T_{u,d}^{\mathrm{leave,osat,G_1}}(k_d)$ (i.e., the time duration that each vehicle in group 1 needs after idling to leave the link), $T_{u,d}^{\mathrm{free,G_1}}(k_d)$ (i.e., the time duration of the free-flow behavior for each vehicle in group 1), $v_{u,d}^{\mathrm{middle,first}}(k_d)$ corresponding to the first vehicle of group 2, and $v_{u,d}^{\mathrm{middle,osat}}(k_d)$ corresponding to the representative vehicle of group 2. For the sake of simplicity, we assume that the traveled distance to the end of the link for all vehicles in group 1 is the same and is equal to $0.5 n_{u,d}^{\mathrm{G_1,osat}}(k_d) l^{\mathrm{veh}}$ (i.e., we assume to have a vertical queue composed of vehicles in group 1).

For the last vehicle in group 1 that will show an accelerating and (possibly a free-flow behavior at the end), using Lemma 3.1 we obtain

$$\frac{n_{u,d}^{\mathrm{G_1,osat}}(k_d) l^{\mathrm{veh}}}{2} = \frac{1}{2} a_{u,d}^{\mathrm{acc}} \left(\frac{v_{u,d}^{\mathrm{free}} - v_{u,d}^{\mathrm{idling}}}{a_{u,d}^{\mathrm{acc}}} \right)^2 + v_{u,d}^{\mathrm{idling}} \left(\frac{v_{u,d}^{\mathrm{free}} - v_{u,d}^{\mathrm{idling}}}{a_{u,d}^{\mathrm{acc}}} \right) + v_{u,d}^{\mathrm{free}} \cdot T_{u,d}^{\mathrm{free,G_1}}(k_d). \tag{125}$$

Moreover, since the leaving flow rate of group 1 in the over-saturated scenario is $\mu_{u,d}$, we can write

$$n_{u,d}^{\mathrm{G_1,osat}}(k_d) = \mu_{u,d} \left(g_{u,d}(k_d) - T_{u,d}^{\mathrm{leave,G_1,osat}}(k_d) \right), \tag{126}$$

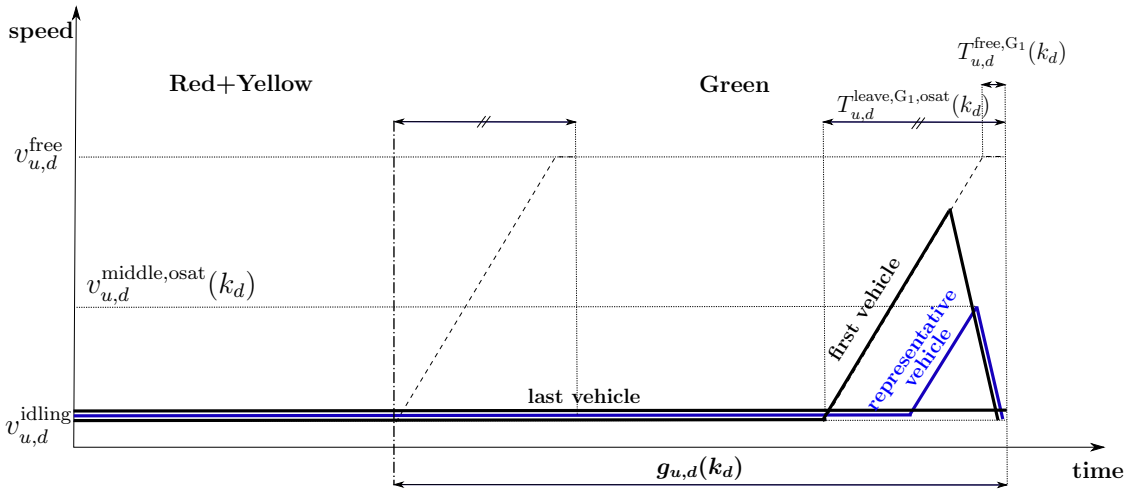

(a) Traffic behaviors for the first, last, and representative vehicle in group 2

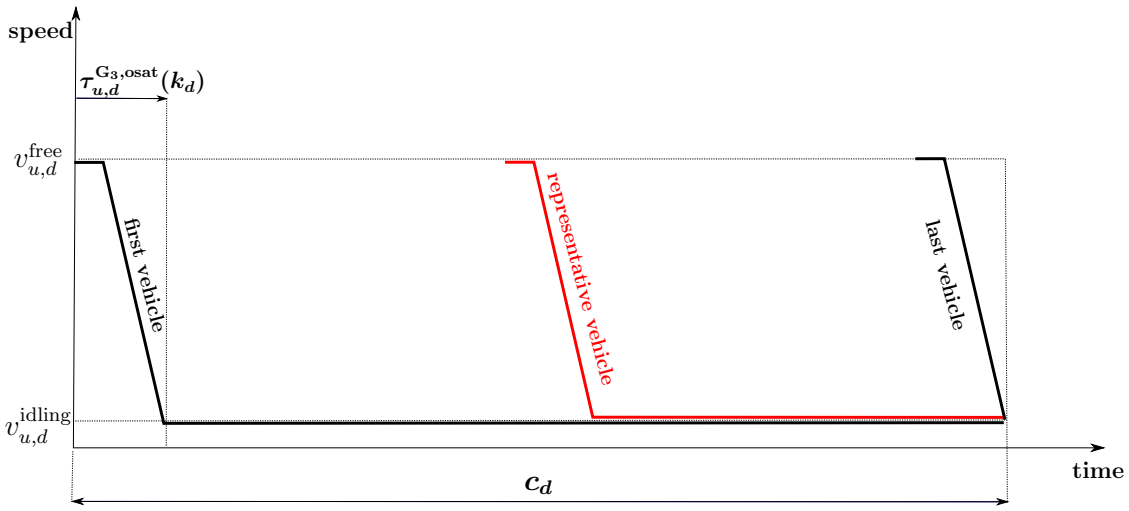

(b) Traffic behaviors for the first, last, and representative vehicle in group 3

Figure 8: Traffic behavior of different groups for **over-saturated** urban traffic scenario

where $g_{u,d}(k_d) - T_{u,d}^{\text{leave,G}_1,\text{osat}}(k_d)$ denotes the temporal distance between the two dashed curves in Figure 8(a). Additionally, from this figure we have

$$T_{u,d}^{\text{leave,G}_1,\text{osat}}(k_d) = \frac{v_{u,d}^{\text{free}} - v_{u,d}^{\text{idling}}}{a_{u,d}^{\text{acc}}} + T_{u,d}^{\text{free,G}_1}(k_d), \tag{127}$$

where from (125), (126), and (127) we obtain

$$T_{u,d}^{\text{leave,G}_1,\text{osat}}(k_d) = \frac{\mu_{u,d} l^{\text{veh}} g_{u,d}(k_d)}{2v_{u,d}^{\text{free}} + \mu_{u,d} l^{\text{veh}}} + \frac{\left(v_{u,d}^{\text{free}} - v_{u,d}^{\text{idling}}\right)^2}{a_{u,d}^{\text{acc}}\left(2v_{u,d}^{\text{free}} + \mu_{u,d} l^{\text{veh}}\right)}, \tag{128}$$

and

$$T_{u,d}^{\text{free,G}_1}(k_d) = \frac{\mu_{u,d} l^{\text{veh}} g_{u,d}(k_d)}{2v_{u,d}^{\text{free}} + \mu_{u,d} l^{\text{veh}}} - \frac{\left(v_{u,d}^{\text{free}} - v_{u,d}^{\text{idling}}\right)\left(\mu_{u,d} l^{\text{veh}} + v_{u,d}^{\text{free}} + v_{u,d}^{\text{idling}}\right)}{a_{u,d}^{\text{acc}}\left(2v_{u,d}^{\text{free}} + \mu_{u,d} l^{\text{veh}}\right)}. \tag{129}$$

For $v_{u,d}^{\text{middle,osat}}(k_d)$, from the time-speed curve of the first vehicle (see Figure 8(a)), we can write

$$T_{u,d}^{\text{leave,G}_1,\text{osat}}(k_d) = \frac{v_{u,d}^{\text{middle,first}}(k_d) - v_{u,d}^{\text{idling}}}{a_{u,d}^{\text{acc}}} + \frac{v_{u,d}^{\text{idling}} - v_{u,d}^{\text{middle,first}}(k_d)}{a_{u,d}^{\text{dec}}}, \tag{130}$$

which gives

$$v_{u,d}^{\text{middle,first}}(k_d) = v_{u,d}^{\text{idling}} + T_{u,d}^{\text{leave,G}_1,\text{osat}}(k_d)\frac{a_{u,d}^{\text{dec}} - a_{u,d}^{\text{acc}}}{a_{u,d}^{\text{dec}} a_{u,d}^{\text{acc}}}, \tag{131}$$

and since $v_{u,d}^{\text{middle,osat}}(k_d)$ is the mean value of $v_{u,d}^{\text{middle,first}}(k_d)$ and $v_{u,d}^{\text{idling}}$, we obtain

$$v_{u,d}^{\text{middle,osat}}(k_d) = v_{u,d}^{\text{idling}} + T_{u,d}^{\text{leave,G}_1,\text{osat}}(k_d)\frac{a_{u,d}^{\text{dec}} - a_{u,d}^{\text{acc}}}{2a_{u,d}^{\text{dec}} a_{u,d}^{\text{acc}}}. \tag{132}$$

Figure 8(b) shows the time-speed curves of the first, last, and representative vehicle of group 3 in the over-saturated scenario. From this figure the free-flow, decelerating, and idling time durations of the representative vehicle are obtained as follows:

- free-flow:

$$\tau_{u,d}^{\text{G}_3,\text{osat}}(k_d) - \frac{v_{u,d}^{\text{idling}} - v_{u,d}^{\text{free}}}{a_{u,d}^{\text{dec}}}; \tag{133}$$

- decelerating:

$$\frac{v_{u,d}^{\text{idling}} - v_{u,d}^{\text{free}}}{a_{u,d}^{\text{dec}}}; \tag{134}$$

- idling:

$$\tau_{u,d}^{\text{G}_3,\text{osat}}(k_d) - \frac{c_d - \tau_{u,d}^{\text{G}_3,\text{osat}}(k_d)}{2}, \tag{135}$$

where $\tau_{u,d}^{\text{G}_3,\text{osat}}(k_d)$ is given by (118).

7 Test example

In this section, we present some results of a simulation-based case study to evaluate the performance of the proposed mesoscopic integrated flow-emission model. As an evaluation platform, we use the traffic microsimulator SUMO (Simulation of Urban MObility) (Krajzewicz et al., 2002, 2012), which is an open-source microscopic traffic flow simulator (continuous-space and discrete-time) developed by the Institute for Transportation Research, German Aerospace Centre (Deutsches Zentrum für Luft- und Raumfahrt, DLR). Since its initial release in 2002, SUMO has evolved into a reliable and versatile platform that provides full-featured simulation and analysis tools for traffic networks (see (Krajzewicz et al., 2012) for more details). Moreover, a remote traffic control interface, called "TraCI" (Wegener et al., 2008), is available, which provides an interface between SUMO and different programming languages including MATLAB for various online running, analysis and control scenarios.

The focus of this paper and the presented case study in this section is on the interface of the macroscopic flow models and microscopic emission models. For this test example, in order to assess the accuracy of the interface, we use SUMO and VT-micro to generate

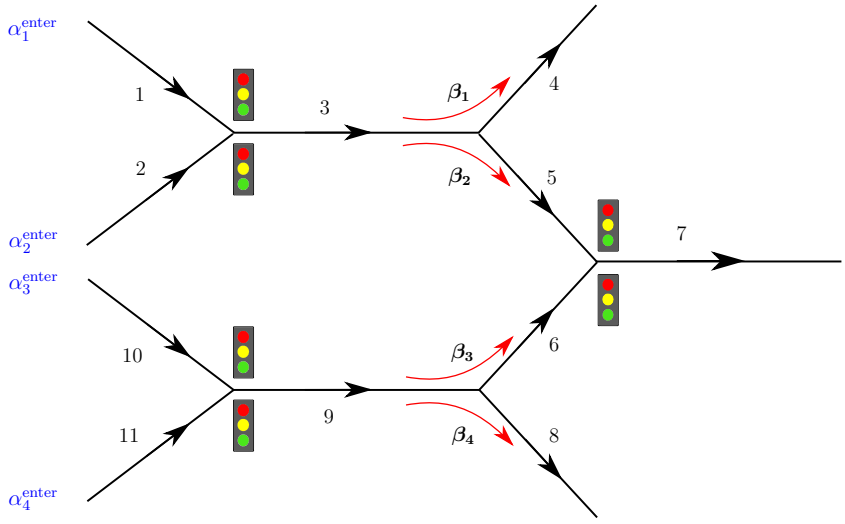

Figure 9: Urban traffic network used for the test example.

both the microscopic and the mesoscopic data. More specifically, for evaluation of the mesoscopic integrated flow-emission model developed via the integrating and interfacing approach proposed in this paper, the urban traffic network represented in Figure 9, which includes 11 single-lane links of length 500 m, four entrances, three exits, and three traffic lights is considered. The entering flows to the network are denoted by $\alpha_i^{\text{enter}},\ i = 1, 2, 3, 4$, and the turning rates (i.e., the percentage of vehicles on a link that intend to turn to a specific downstream link) $\beta_1,\ \beta_2,\ \beta_3$, and β_4 are assumed to be 0.4, 0.6, 0.4, and 0.6. Note that β_1 and β_2 are the turning rates for the vehicles on link 3 to, respectively, link 4 and link 5, and that β_3 and β_4 are the turning rates for the vehicles on link 9 to, respectively, link 6 and link 8 (see Figure 9).

The traffic network shown in Figure 9 was modeled in SUMO, where the measurements obtained from SUMO were coupled with the microscopic emission model, VT-micro explained in Section 2. VT-micro is selected here because it can provide the instantaneous emissions of CO, HC, and NO_x based on both the speed and the acceleration of individual vehicles in the traffic network. Before we start to implement the proposed model, we should identify the parameters of the model by solving an offline identification optimization problem. For identifying the parameters and for computation of the emissions by the proposed mesoscopic integrated flow-emission model, VT-micro was used to compute (6). An extensive data set was collected by running various traffic scenarios in SUMO. The demand profiles, the cycle time and the green times of the traffic lights, and the turning rates of the links are the inputs. The data that should be collected includes the total number of vehicles on each link within the network and the number of vehicles waiting in the queue on each link. The total emissions of CO, HC, and NO_x computed by VT-micro based on the flow data captured by SUMO are the outputs. Moreover, the set of parameters that should be identified include the traffic parameters, in particular, the free-flow and the idling speed, the acceleration and deceleration, the link capacities, the saturated leaving flow rates (i.e., the maximum possible discharge rates) of the links, and the average vehicle length in the network. Then an optimization problem was formulated that minimizes the relative error of the produced emissions via the proposed model w.r.t. the computed emissions by SUMO and VT-micro, with the parameter vector considered as the optimization variable. We used the "lsqnonlin" solver with the "trust-region-reflective" algorithm in MATLAB to find the parameters. The parameter values found via model identification

Table 1: Identified traffic parameters for the emissions of CO using SUMO.

v^{free} [m/s]	v^{idling} [m/s]	a^{acc} [m/s^2]	a^{dec} [m/s^2]	C [veh]	μ [veh/s]	l^{veh} [m]
11.8	0.1	1.60	-1.80	14.3	0.9	5.4

Table 2: Identified traffic parameters for the emissions of HC using SUMO.

v^{free} [m/s]	v^{idling} [m/s]	a^{acc} [m/s^2]	a^{dec} [m/s^2]	C [veh]	μ [veh/s]	l^{veh} [m]
16.9	0.1	1.99	-1.25	71.6	4.9	3.5

Table 3: Identified traffic parameters for the emissions of NO_x using SUMO.

v^{free} [m/s]	v^{idling} [m/s]	a^{acc} [m/s^2]	a^{dec} [m/s^2]	C [veh]	μ [veh/s]	l^{veh} [m]
13.8	0.1	1.36	-1.05	62.7	3.8	5.7

for the emissions of CO, HC, and NO_x are given [9] in Tables 1, 2, and 3.

Remark. Note that the identified values of the traffic parameters may differ from their real physical values as a result of the assumptions and simplifications made for developing the mathematical model. In particular, in addition to the dynamic variables such as the speeds and the acceleration and deceleration, we should also identify other parameters such as the link capacities to minimize the mismatch between the two mesoscopic and microscopic models.

To evaluate the performance of the proposed model, new traffic scenarios that are different from those used for model identification were simulated in SUMO. The total number of vehicles in each link and the number of vehicles standing in the queue in each link were extracted from SUMO. Then for each link, the average value of the total number of vehicles and the average value of the queue length were computed per model time step (i.e., per cycle time of the traffic lights, which is 60 s in our simulations).

Figures 10(a) and 10(b) show the demand profiles (i.e., α_i^{enter}, $i = 1, 2, 3, 4$) for two different traffic scenarios, where the first scenario corresponds to a lower demand and the second scenario corresponds to a higher demand. Note that for this scenario the green times of the three traffic lights shown in Figure 9 are assumed to be 30 s. For these two cases, we could model the three cases (under-saturated, saturated, and over-saturated) in the entering and middle links of the network shown in Figure 9. The instantaneous speed and the instantaneous acceleration profiles of the individual vehicles within the network were extracted from SUMO for the two given cases, and the emissions of CO, HC, and NO_x produced by each vehicle were computed using VT-micro. Summing up these individual values, the total emissions of CO, HC, and NO_x by the vehicles for the entire simulated period were obtained. These results were used as a reference point for evaluation of the emission values computed via the proposed mesoscopic flow-emission model using the parameter values given in Tables 1, 2, and 3 for, respectively, the emissions of CO, the emissions of HC, and the emissions of NO_x, and for the same input vector (including the demand at the entrances, the green time of the traffic lights, the total number of vehicles on each link, etc.).

Figures 11(a), 12(a), and 13(a) show the relative error in percentage of the instantaneous emissions of CO, HC, and NO_x as a function of the time step for case 1 for the entire network computed by the proposed integrated flow-emission model w.r.t. the in-

[9] To identify the parameters of the model for the case study, we have considered the same acceleration and deceleration rates for the under-saturated, saturated, and over-saturated traffic scenarios (in order to reduce the number of parameters that should be determined via the identification optimization problem). However, since this optimization problem is solved offline, one can consider different acceleration and deceleration rates that may possibly result in more accurate results.

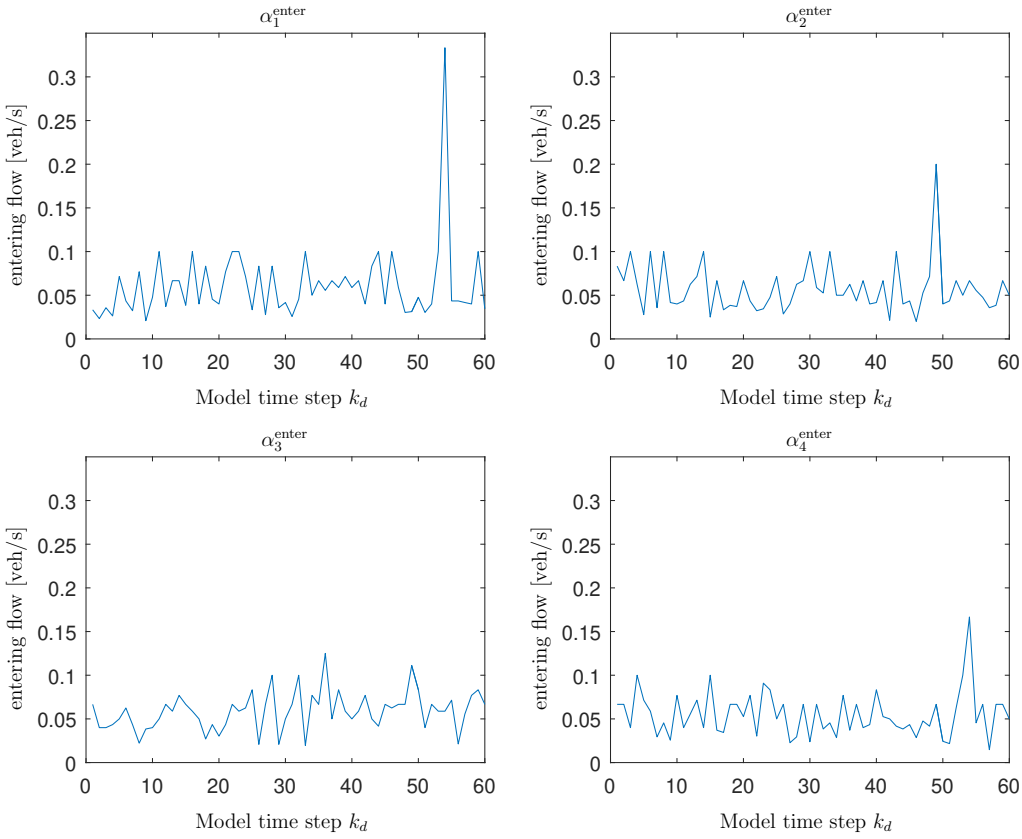

(a) Demand profiles (case 1) for a 1-hour simulation (the green times are 30 s).

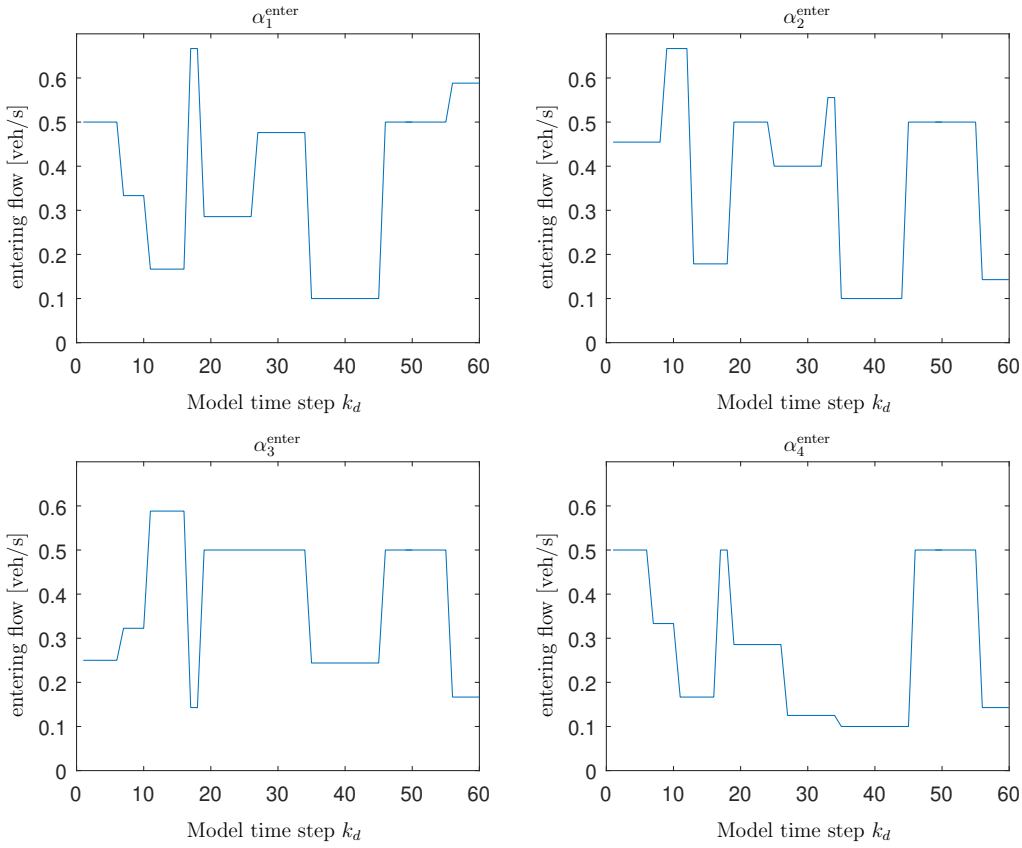

(b) Demand profiles (case 2) for a 1-hour simulation (the green times are 30 s).

Figure 10: Demand profiles for the case study (case 1: low demand, case 2: high demand).

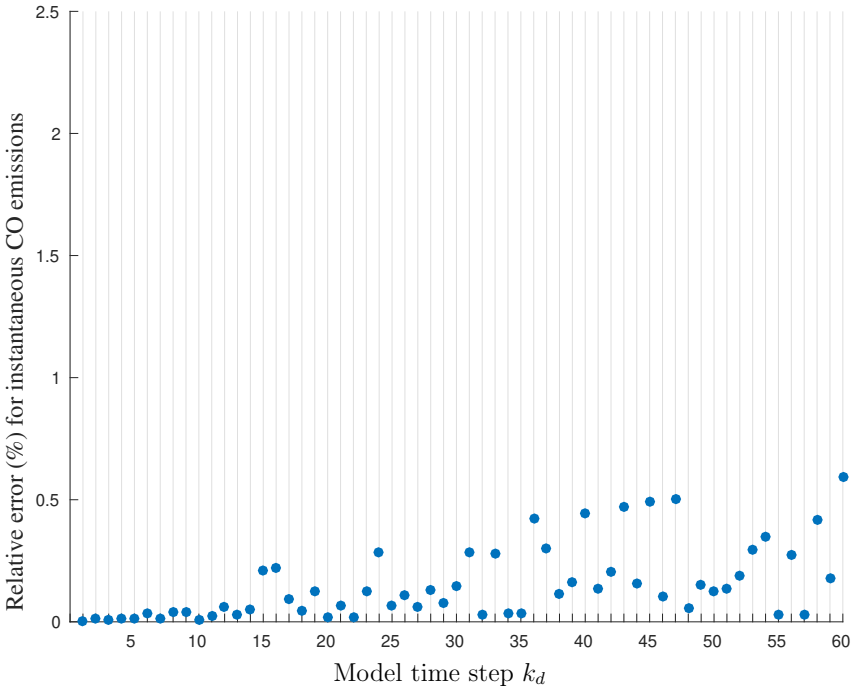

(a) Relative errors (%) of the instantaneous CO emissions computed for demand profiles of case 1 using the integrating and interfacing approach proposed in this paper and by the combined SUMO and VT-micro model.

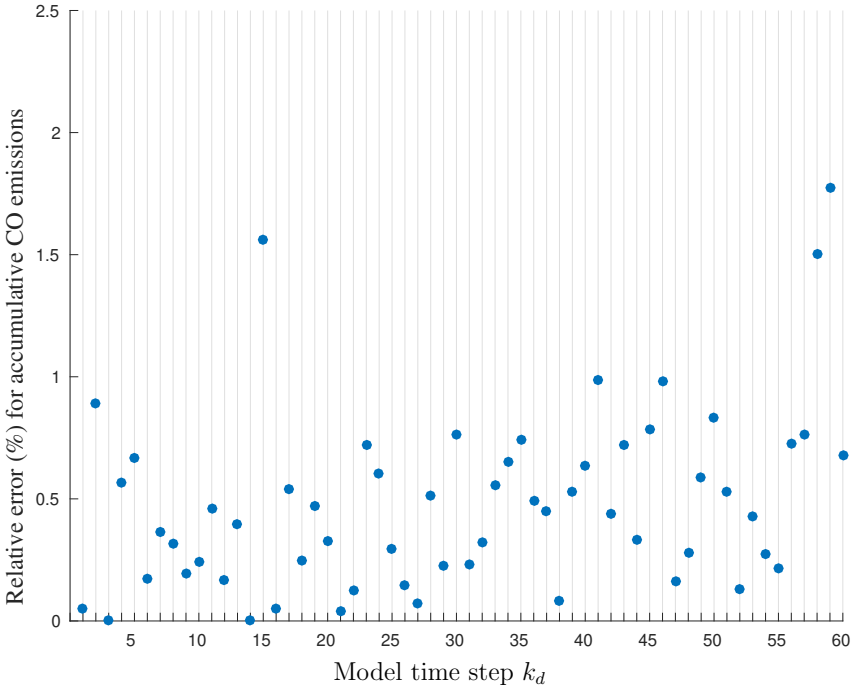

(b) Relative errors (%) of the accumulative CO emissions computed for demand profiles of case 1 using the integrating and interfacing approach proposed in this paper and by the combined SUMO and VT-micro model.

Figure 11: Results for CO emissions for case 1.

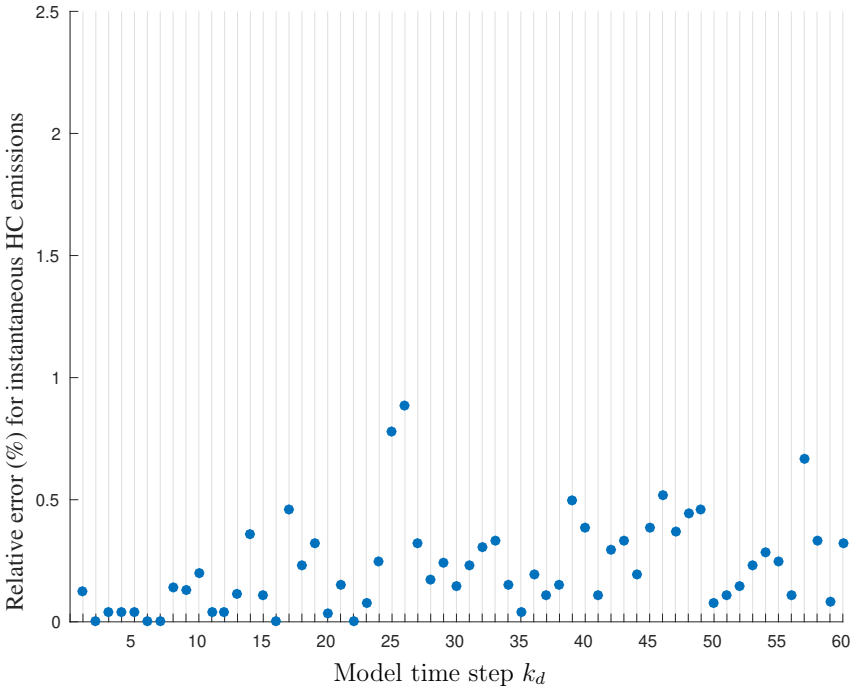

(a) Relative errors (%) of the instantaneous HC emissions computed for demand profiles of case 1 using the integrating and interfacing approach proposed in this paper and by the combined SUMO and VT-micro model.

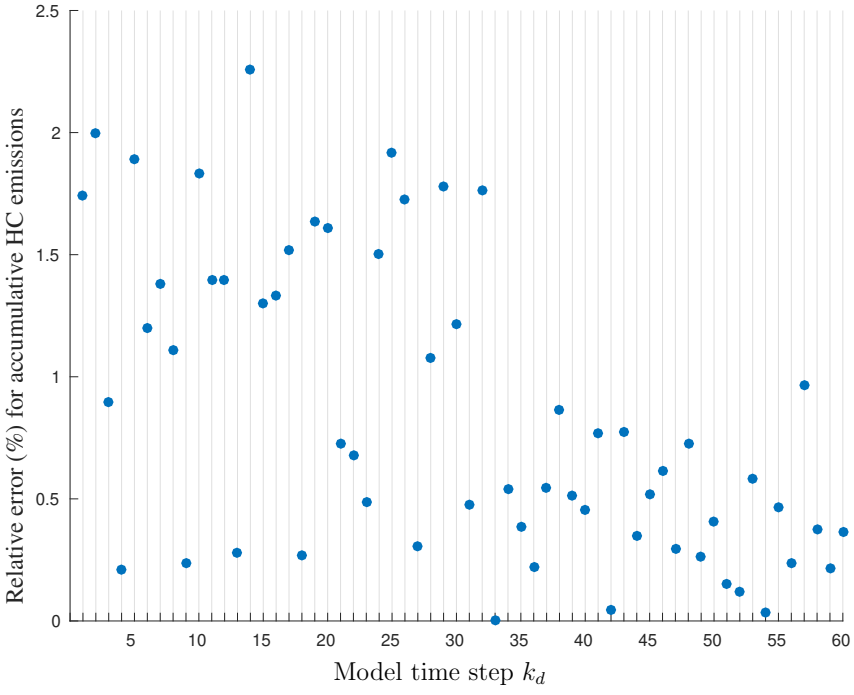

(b) Relative errors (%) of the accumulative HC emissions computed for demand profiles of case 1 using the integrating and interfacing approach proposed in this paper and by the combined SUMO and VT-micro model.

Figure 12: Results for HC emissions for case 1.

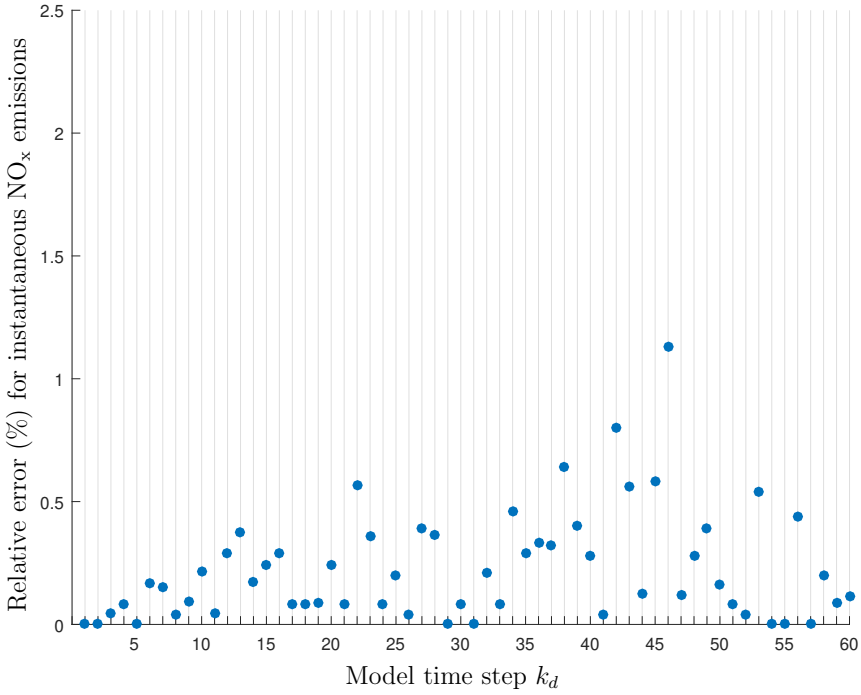

(a) Relative errors (%) of the instantaneous NO_x emissions computed for demand profiles of case 1 using the integrating and interfacing approach proposed in this paper and by the combined SUMO and VT-micro model.

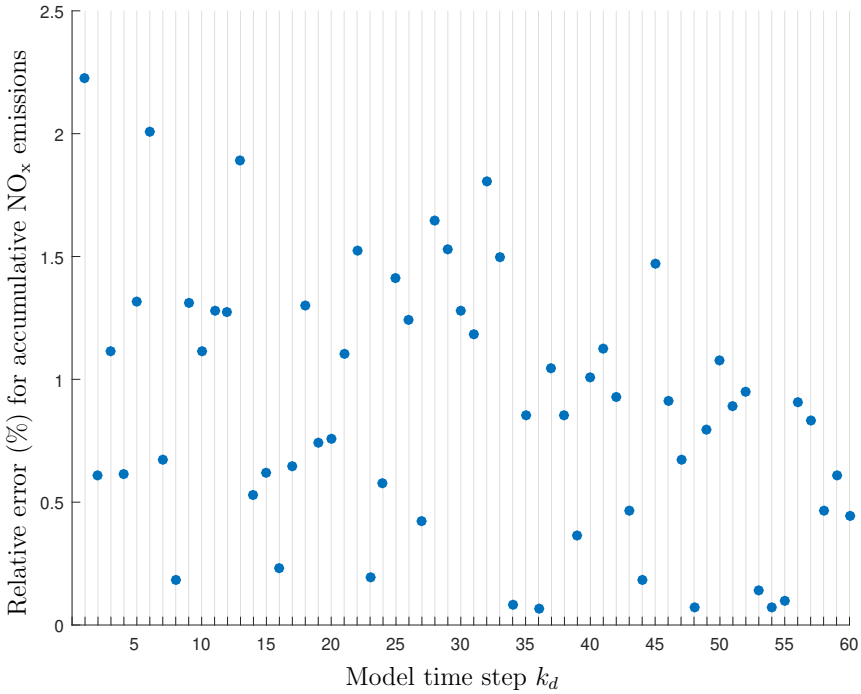

(b) Relative errors (%) of the accumulative NO_x emissions computed for demand profiles of case 1 using the integrating and interfacing approach proposed in this paper and by the combined SUMO and VT-micro model.

Figure 13: Results for NO_x emissions for case 1.

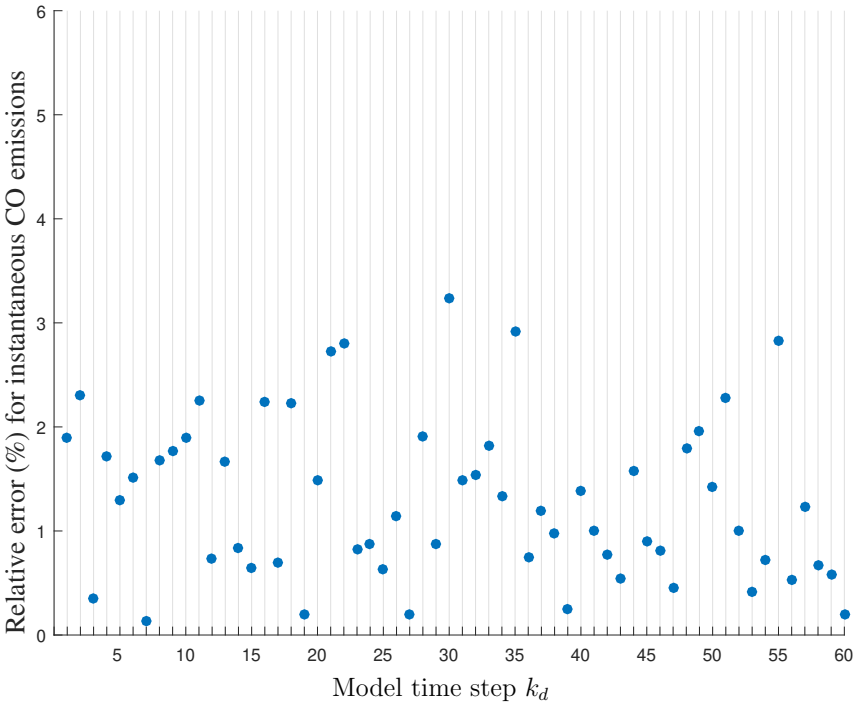

(a) Relative errors (%) of the instantaneous CO emissions computed for demand profiles of case 2 using the integrating and interfacing approach proposed in this paper and by the combined SUMO and VT-micro model.

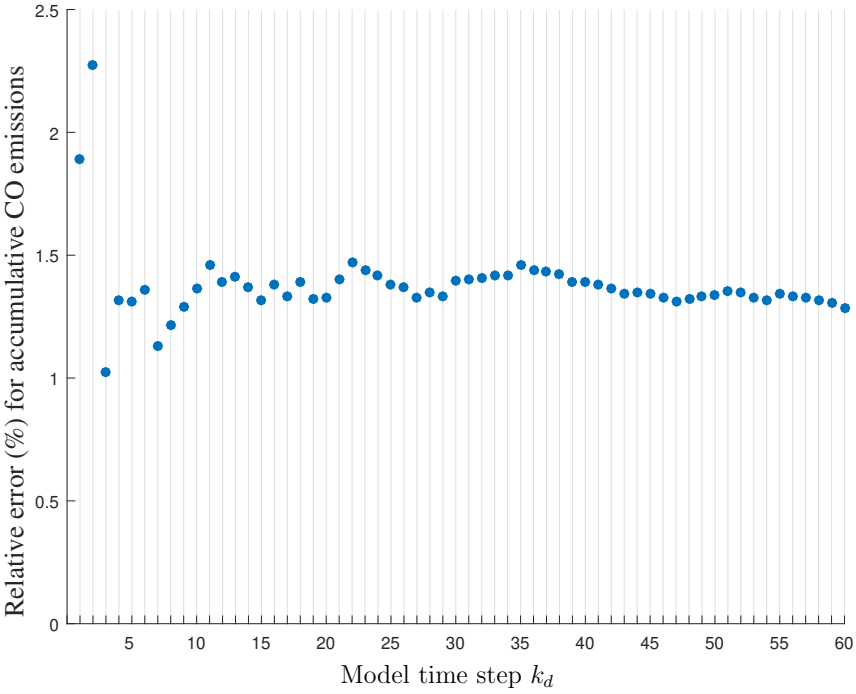

(b) Relative errors (%) of the accumulative CO emissions computed for demand profiles of case 2 using the integrating and interfacing approach proposed in this paper and by the combined SUMO and VT-micro model.

Figure 14: Results for CO emissions for case 2.

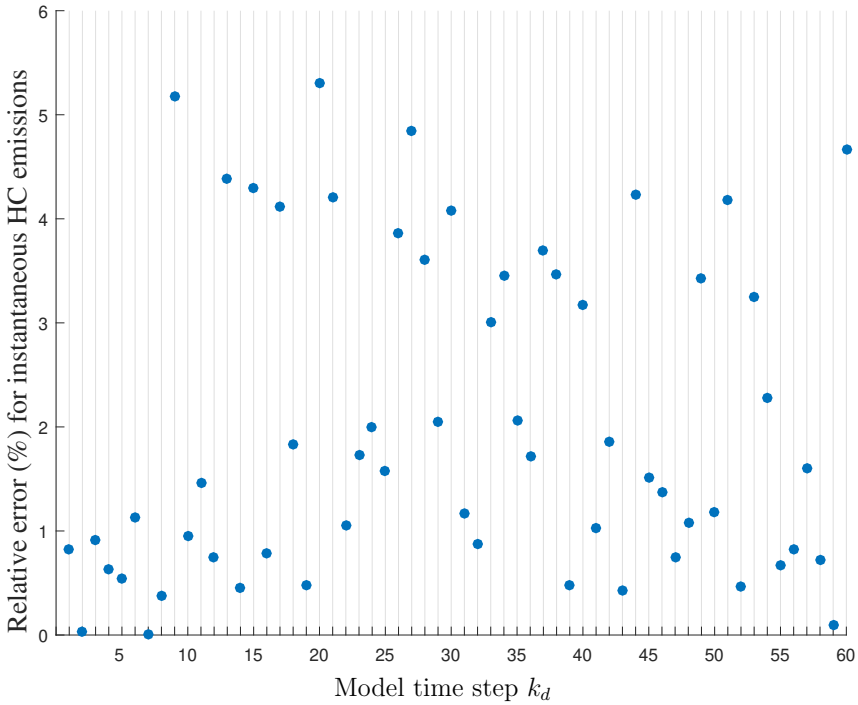

(a) Relative errors (%) of the instantaneous HC emissions computed for demand profiles of case 2 using the integrating and interfacing approach proposed in this paper and by the combined SUMO and VT-micro model.

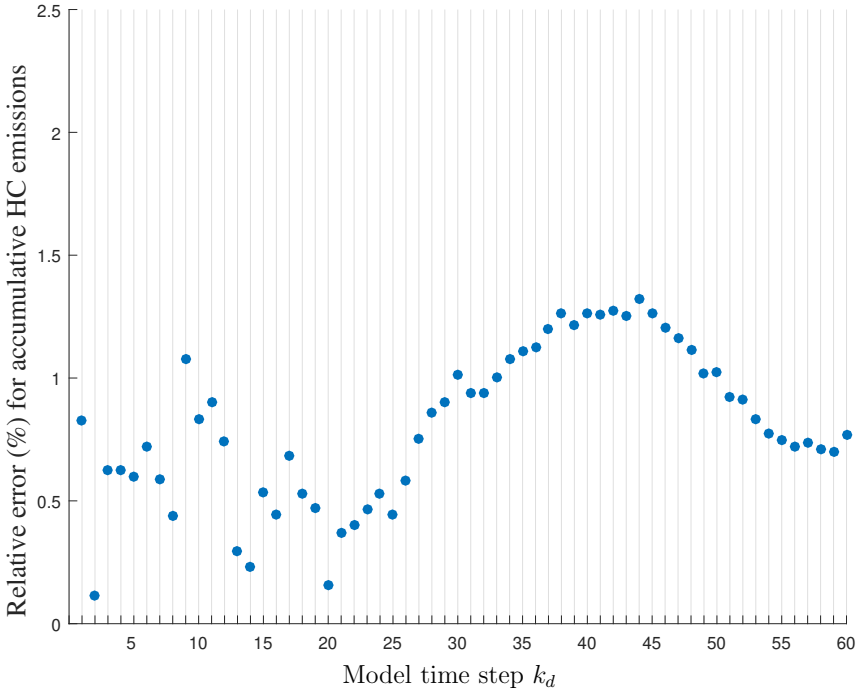

(b) Relative errors (%) of the accumulative HC emissions computed for demand profiles of case 2 using the integrating and interfacing approach proposed in this paper and by the combined SUMO and VT-micro model.

Figure 15: Results for HC emissions for case 2.

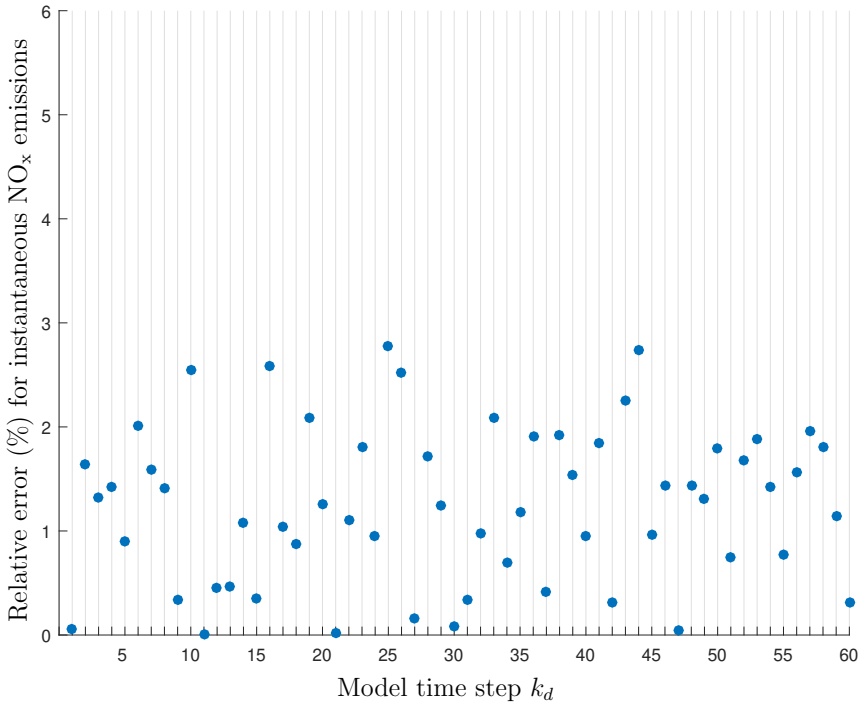

(a) Relative errors (%) of the instantaneous NO_x emissions computed for demand profiles of case 2 using the integrating and interfacing approach proposed in this paper and by the combined SUMO and VT-micro model.

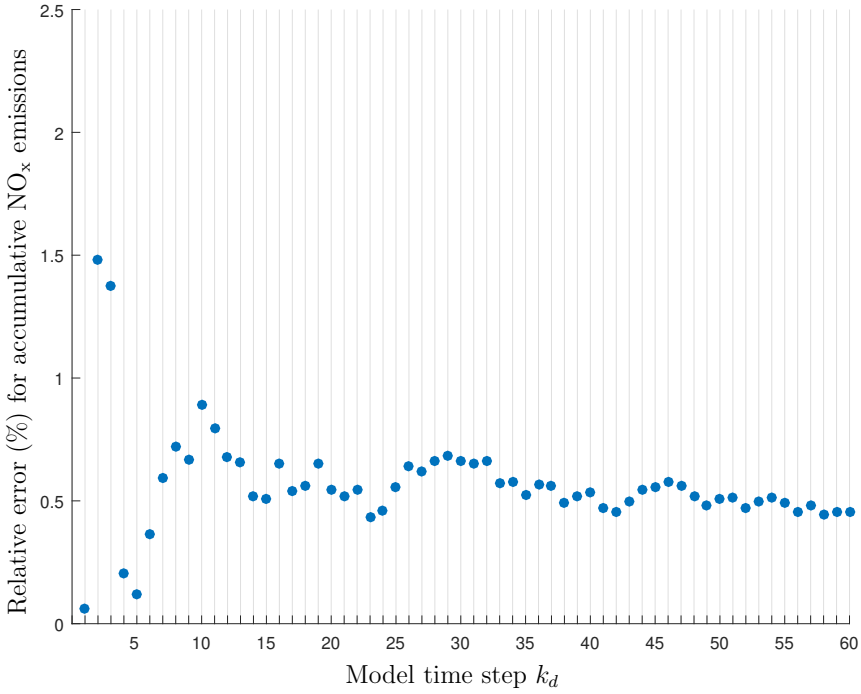

(b) Relative errors (%) of the accumulative NO_x emissions computed for demand profiles of case 2 using the integrating and interfacing approach proposed in this paper and by the combined SUMO and VT-micro model.

Figure 16: Results for NO_x emissions for case 2.

stantaneous emissions captured from SUMO combined with VT-micro versus time for one hour of simulation. This relative error for the pollutant $\theta \in \{\mathrm{CO}, \mathrm{HC}, \mathrm{NO_x}\}$ is defined by

$$e_\theta^{\mathrm{rel}} = \frac{\left|\mathrm{TE}_\theta^{\mathrm{model}} - \mathrm{TE}_\theta^{\mathrm{microsimulator}}\right|}{\mathrm{TE}_\theta^{\mathrm{microsimulator}}}. \tag{136}$$

Table 4 summarizes the results of the simulations for the instantaneous emissions. From this table, the relative error of the instantaneous emissions of CO has a mean value of 0.152 %, a standard deviation of 0.149, and a maximum of 0.593 %. The mean value, the standard deviation, and the maximum value of the instantaneous emissions of HC are, respectively, 0.226 %, 0.189, and 0.884 %. For the instantaneous emissions of $\mathrm{NO_x}$, the mean value of the relative error is 0.226 %, the standard deviation of the relative error is 0.223, and its maximum value is 1.13 %.

Figures 11(b), 12(b), and 13(b) show the relative error in percentage of the accumulative total emissions of CO, HC, and $\mathrm{NO_x}$ (which is the sum of the instantaneous emissions from the first time step till the current time step) for case 1 w.r.t. the emissions computed via SUMO and VT-micro. From these figures, Table 5 was extracted, which shows that the relative error of the accumulative emissions of CO during a 1-hour simulation does not exceed 2 %, where this relative error has a mean value and a standard deviation of, respectively, 0.483 % and 0.368. For the accumulative total emissions of HC, the mean value and the standard deviation of the relative error are, respectively, 0.848 % and 0.617, while the relative error is always less than 2.5 %. Finally, from Figure 13(b), for the accumulative total emissions of $\mathrm{NO_x}$, the mean value is 0.887 %, the standard deviation is 0.617, and the relative error does not go higher than 2.5 %. These results prove the excellent accuracy provided by the mesoscopic integrated flow-emission model, which is based on the integrating and interfacing approach proposed in this paper.

Moreover, the results corresponding to case 2 are shown in Figures 14(a), 15(a), and 16(a), which illustrate the relative error in percentage of the instantaneous emissions of CO, HC, and $\mathrm{NO_x}$ as a function of the time step, and also in Figures 14(b), 15(b), and 16(b), which show the relative error in percentage of the accumulative total emissions of CO, HC, and $\mathrm{NO_x}$. These results are summarized in Tables 6 and 7, where we can see that the relative error of the instantaneous emissions of CO, HC, and $\mathrm{NO_x}$ is less than, respectively, 3.233 %, 5.310 %, and 2.778 %. Additionally, the standard deviations of the relative errors are always less than 1.6. For the relative error of the accumulative emissions of CO, HC, and $\mathrm{NO_x}$, the relative error does not exceed 2.3 %, the mean value of the relative error is less than 1.4 %, and the standard deviation is below 0.32.

8 Conclusions and future work

In this paper, we have proposed a general framework to integrate and interface traffic flow and emission models. Using the proposed approach, a mesoscopic integrated flow-emission traffic model is generated, which considers an aggregated behavior for groups of vehicles instead of considering the behavior of individual vehicles, and that provides a high accuracy and a low computation time. The proposed approach can integrate any traffic flow model that updates the total number of vehicles in the links and the number of vehicles in the queues on the links at every model time step, and any microscopic emission model that takes into account the individual speed and acceleration of vehicles in the network.

The resulting mesoscopic integrated flow-emission models are, on the one hand, fast enough for real-time computations due to their mesoscopic nature. On the other hand, the

Table 4: Mean and standard deviation of the relative error of the instantaneous emissions for case 1 (low demand).

	mean of the relative error (%)	standard deviation of the relative error	maximum of the relative error (%)
TE_{CO}	0.152	0.149	0.593
TE_{HC}	0.226	0.189	0.884
TE_{NO_x}	0.226	0.223	1.130

Table 5: Mean and standard deviation of the relative error of the accumulative emissions for case 1 (low demand).

	mean of the relative error (%)	standard deviation of the relative error	maximum of the relative error (%)
TE_{CO}	0.483	0.368	1.776
TE_{HC}	0.848	0.617	2.260
TE_{NO_x}	0.887	0.525	2.226

Table 6: Mean and standard deviation of the relative error of the instantaneous emissions for case 2 (high demand).

	mean of the relative error (%)	standard deviation of the relative error	maximum of the relative error (%)
TE_{CO}	1.303	0.772	3.233
TE_{HC}	2.036	1.542	5.310
TE_{NO_x}	1.255	0.746	2.778

Table 7: Mean and standard deviation of the relative error of the accumulative emissions for case 2 (high demand).

	mean of the relative error (%)	standard deviation of the relative error	maximum of the relative error (%)
TE_{CO}	1.377	0.154	2.273
TE_{HC}	0.810	0.313	1.322
TE_{NO_x}	0.566	0.209	1.481

resulting models provide a high level of accuracy for computation of the total emissions and the total fuel consumption of the vehicles compared with microscopic traffic models, based on the results of a case study presented in this paper. The results of the case study show that the relative error (in percentage) of the instantaneous total emissions of the vehicles computed by the mesoscopic integrated flow-emission model generated via the proposed approach w.r.t. the instantaneous total emissions found via the microsimulation traffic software SUMO and the microscopic emission model VT-micro does not exceed 5.3 % for CO, HC, and NO_x. Moreover, the mean value and the standard deviation of the relative error are, respectively, less than 2 % and 1.6 for CO, HC, and NO_x. Moreover, the relative error (%) of the accumulative total emissions of the vehicles for the mesoscopic integrated flow-emission model w.r.t. SUMO and VT-micro does not exceed 2.3 % for CO, HC, and NO_x. The mean value of the relative error is less than 1.4 %, and the standard deviation is less than 0.7.

As a topic for future work, due to the resulting low computation time and high accuracy, the proposed integrating and interfacing approach can be used to generate mesoscopic integrated flow-emission models appropriate for (real-time) model-based traffic applications. An important potential application for the resulting mesoscopic model is to use it as the internal prediction model of a model-predictive controller that may have different control purposes, such as reduction of the traffic congestion and emissions via traffic signal control, route guidance, etc. More extensive assessment of the proposed integrating and interfacing approach can be done for further set-ups, scenarios, and traffic signal control strategies. An extensive and in-depth sensitivity analysis of the results produced by the model w.r.t. the parameters used in the model is another topic for future work. Moreover, we will also consider combinations of other macroscopic traffic flow models and microscopic emission models. In addition to that, further investigation and research on different levels of aggregation for urban traffic flow models and traffic emission models is of interest.

Acknowledgments

This research has been supported by the European COST Action TU1102 and by the NWO-NSFC project "Multi-level predictive traffic control for large-scale urban networks" (629.001.011), which is partly financed by the Netherlands Organization for Scientific Research (NWO). For the second and the third author, the research leading to these results has received funding from the European Commission under the European Union's Seventh Framework Programme (FP/2007-2013) / FP7-ICT-2013.3.4, project LOCAL4GLOBAL (n. 611538). We are also very grateful to Yu Hu for his assistance in performing the simulations within SUMO.

References

K. Aboudolas, M. Papageorgiou, A. Kouvelas, and E. Kosmatopoulos. A rolling-horizon quadratic-programming approach to the signal control problem in large-scale congested urban road networks. *Transportation Research Part C*, 18(5):680–694, 2010.

K. Ahn, A. Trani, H. Rakha, and M. van Aerde. Microscopic fuel consumption and emission models. In *Proceedings of the* 78$^{\text{th}}$ *Annual Meeting of the Transportation Research Board*, Washington DC, USA, June–July 1999.

W. P. Anderson, S. K. Pavlos, E. J. Miller, and R. Buliung. Simulating automobile emissions in an integrated urban model. *Transportation Research Record*, 1520:71–80, 1996.

M. Barth and K. Boriboonsomsin. Real-world carbon dioxide impacts of traffic congestion. *Transportation Research Record*, 2058:163–171, 2008.

M. Barth, F. An, J. Norbeck, and M. Ross. Modal emissions modeling: A physical approach. *Transportation Research Record*, 1520:81–88, 1996.

T. Bellemans, B. De Schutter, and B. De Moor. Model predictive control for ramp metering of motorway traffic: A case study. *Control Engineering Practice*, 14(7):757–767, 2006.

Center for Economics and Business Research. The future economic and environmental costs of gridlock in 2030. Technical report, INRIX, July 2014.

K. Chen and L. Yu. Microscopic traffic-emission simulation and case study for evaluation of traffic control strategies. *Journal of Transportation Systems Engineering and Information Technology*, 7(1):93–99, 2007.

A. Csikós, T. Tettamanti, and I. Varga. Macroscopic modeling and control of emission in urban road traffic networks. *Transport*, 30(2):152–161, 2015.

C. Diakaki, M. Papageorgiou, and K. Aboudolas. A multivariable regulator approach to traffic-responsive network-wide signal control. *Control Engineering Practice*, 10(2): 183–195, 2002.

C. Diakaki, V. Dinopoulou, K. Aboudolas, M. Papageorgiou, E. Ben-Shabat, E. Seider, and A. Leibov. Extensions and new applications of the traffic-responsive urban control strategy: Coordinated signal control for urban networks. *Transportation Research Record*, 1856:202–211, 2003.

D. Gazis, R. Herman, and R. Rothery. Nonlinear follow the leader models of traffic flow. *Operations Research*, 9(4):545–567, 1961.

S. Gori, S. La Spada, L. Mannini, and M. Nigro. A dynamic mesoscopic emission model for signalized intersections. In *Proceedings of the* 16$^{\text{th}}$ *International IEEE Conference on Intelligent Transportation Systems (ITSC 2013)*, pages 2212–2217, The Hague, The Netherlands, Oct. 6-9, 2013.

S. P. Hoogendoorn and P. H. L. Bovy. State-of-the-art of vehicular traffic flow modelling. *Proceedings of the Institution of Mechanical Engineers, Part I: Journal of Systems and Control Engineering*, 215(4):283–303, 2001.

D. Krajzewicz, G. Hertkorn, C. Rösel, and P. Wagner. SUMO (Simulation of Urban MObility); An open-source traffic simulation. In *Proceedings of the* 4$^{\text{th}}$ *Middle East Symposium on Simulation and Modelling (MESM'02)*, pages 183–187, Sharjah, United Arab Emirates, Sept. 2002.

D. Krajzewicz, J. Erdmann, M. Behrisch, and L. Bieker. Recent development and applications of SUMO - Simulation of Urban MObility. *International Journal on Advances in Systems and Measurements*, 5(3–4):128–138, 2012.

N. E. Ligterink, R. De Lange, and E. Schoen. Refined vehicle and driving-behaviour dependencies in the VERSIT+ emission model. In *Proceedings of the ETAPP Symposium*, pages 177–186, Toulouse, France, June 2009.

S. Lin, B. De Schutter, Y. Xi, and H. Hellendoorn. Efficient network-wide model-based predictive control for urban traffic networks. *Transportation Research Part C*, 24:122–140, oct 2012.

S. Lin, B. De Schutter, Y. Xi, and H. Hellendoorn. Integrated urban traffic control for the reduction of travel delays and emissions. *IEEE Transactions on Intelligent Transportation Systems*, 1(4):1609–1619, 2013.

J. Maciejowski. *Predictive Control with Constraints*. Prentice Hall, London, UK, 2002.

A. Messmer and M. Papageorgiou. METANET: A macroscopic simulation program for motorway networks. *Traffic Engineering and Control*, 31(9):466–470, 1990.

L. Ntziachristos, D. Gkatzoflias, K. Chariton, and Z. Samaras. *COPERT: A European Road Transport Emission Inventory Model Information Technologies in Environmental Engineering*. Springer, Berlin, Heidelberg, 2009.

A. Paz, V. Molano, E. Martinez, C. Gaviria, and C. Arteaga. Calibration of traffic flow models using a memetic algorithm. *Transportation Research Part C*, 55:432–443, 2015.

L. A. Pipes. An operational analysis of traffic dynamics. *Journal of Applied Physics*, 24 (3):274–281, 1953.

Y. G. Qi, H. H. Teng, and L. Yu. Microscale emission models incorporating acceleration and deceleration. *Journal of Transport Engineering*, 130(3):348–359, 2004.

H. Rakha, H. Yue, and F. Dion. VT-meso model framework for estimating hot-stabilized light-duty vehicle fuel consumption and emission rates. *Canadian Journal of Civil Engineering*, 38(11):1274–1286, 2011.

A. Sjodin, K. Persson, K. Andreasson, B. Arlander, and B. Galle. On-road emission factors derived from measurements in a traffic tunnel. *International Journal of Vehicle Design*, 20(1–4):147–158, 1998.

M. van den Berg, A. Hegyi, B. De Schutter, and J. Hellendoorn. Integrated traffic control for mixed urban and freeway networks: A model predictive control approach. *European Journal of Transport and Infrastructure Research*, 7(3):223–250, September 2007.

A. Wegener, M. Piórkowski, M. Raya, H. Hellbrück, S. Fischer, and J. P. Hubaux. TraCI: An interface for coupling road traffic and netwok simulators. In *Proceedings of the* 11$^{\text{th}}$ *Communications and Networking Simulation Symposium (CNS'08)*, pages 155–163, New York, USA, 2008.

S. K. Zegeye. *Model-Based Traffic Control for Sustainable Mobility*. PhD thesis, Delft University of Technology, Oct. 2011.

S. K. Zegeye, B. De Schutter, J. Hellendoorn, and E. A. Breunesse. Reduction of area-wide emissions using an efficient model-based traffic control strategy. In *Proceedings of the 2011 IEEE Forum on Integrated and Sustainable Transportation Systems (FISTS 2011)*, pages 307–312, Vienna, Austria, June–July 2011.